Third-Order Consensus for Robust Distributed Formation Control of Double Integrator Vehicles

Pedro Trindade, Pedro Batista, and Rita Cunha

Control Engineering Practice, vol. 133, 105436, April 2023

https://doi.org/10.1016/j.conengprac.2023.105436

Cite as: Pedro Trindade, Pedro Batista, and Rita Cunha, "Third-Order Consensus for Robust Distributed Formation Control of Double Integrator Vehicles," Control Engineering Practice, vol. 133, 105436, April 2023.

Control Engineering Practice 133 (2023) 105436

Contents lists available at ScienceDirect

Control Engineering Practice

journal homepage: www.elsevier.com/locate/conengprac

Third-order consensus for robust distributed formation control of double integrator vehicles

Pedro Trindade *, Pedro Batista, Rita Cunha

Institute for Systems and Robotics, LARSyS, Instituto Superior Técnico, Universidade de Lisboa, Portugal

ARTICLE INFO

Keywords:
Formation control
Third-order consensus
Convergence criteria
Disturbance rejection
Multirotor vehicles

ABSTRACT

This paper presents the development of a robust distributed and cooperative control algorithm for formation tracking by teams of vehicles modeled as double integrators, and exemplifies its use through the application to multirotor vehicles. To achieve coordination between the vehicles in a distributed manner, in the sense that only local information is either exchanged or perceived, consensus-based protocols are considered. Consensus protocols for agents modeled with up to three integrators are presented, and the third-order protocol is analyzed under any time-invariant sensing or communication topology. The analysis seeks to determine exact bounds on the coupling gains of the protocol that lead to convergence. To that end, an extension of the Routh–Hurwitz criterion to polynomials with complex coefficients is used, leading to novel necessary and sufficient conditions for convergence. Moreover, these novel bounds turn out to be a generalization of the ones described in the literature for second-order consensus, as the latter can be recovered as a special case. The effect of disturbances acting upon the agents is also analyzed and related to their ability to achieve robust consensus in the sense that bounded disturbances do not lead to instability. Further results are derived for the case of constant disturbances, a special case that is particularly relevant for formation control. The third-order consensus protocol is then explored to incorporate integral action in a formation tracking controller used for double integrator vehicles and thereby enable constant disturbance rejection. Finally, experiments resulting from the application of the proposed control algorithms to multirotor vehicles are presented, in order to validate the analysis and demonstrate the usefulness of this approach.

1. Introduction

Formation control is an important topic of research in the coordinated motion of multiple unmanned autonomous vehicles. Moving in formation can have several advantages on the overall system, such as increased redundancy and robustness, and reduced cost. However, this problem presents several challenges, mainly related to the lack of total information by each agent, but also to the desire to use a decentralized approach. In decentralized approaches, each agent makes its own decisions based solely on local information, therefore a central controller, coordinator or supervisor does not exist, making the problem more challenging. Despite the challenges, a decentralized approach is still the one that presents more potential applications, since it provides scalability and robustness to the system.

A survey on the topic of multi-agent formation control can be found in the work by Oh et al. (2015). There, the authors divide the formation control approaches into three categories, based mainly on the amount of interactions needed and on the sensing capabilities of the vehicles. These categories are the position-, displacement-, and distance-based approaches. The position-based approach considers that each agent has access to measurements in the inertial frame (e.g. absolute position measurements). In this case, each agent can be equipped with a control law to drive its position to a desired position, thus achieving the prescribed formation without the need to interact with others. This is, however, the most demanding approach in terms of the sensing capability of each agent. The displacement-based approach considers that the vehicles can only measure relative quantities (e.g., measurement of the relative position or displacement to another vehicle), and that they have a common reference for orientation. More interactions between agents are thus required in order to overcome the reduced sensing capability. For agents modeled as single integrators, this approach is studied under directed interaction topologies, for example, by Ren et al. (2004), considering consensus-based protocols. For the case of agents modeled as double integrators, it was studied, for example, by Ren and Atkins (2007) and Han et al. (2017). Finally, in the distance-based approach, it is assumed that agents only have access to relative measurements and do not share a sense of orientation. Formations are stabilized based only on the distance between the agents, not accounting for the orientation of the formation. This approach is the less demanding in terms of sensing capability of the agents. However, it requires the use

* Corresponding author.
E-mail addresses: pedro.trindade@isr.tecnico.ulisboa.pt (P. Trindade), pbatista@isr.tecnico.ulisboa.pt (P. Batista), rita@isr.tecnico.ulisboa.pt (R. Cunha).

https://doi.org/10.1016/j.conengprac.2023.105436
Received 24 May 2022; Received in revised form 3 December 2022; Accepted 10 January 2023
Available online 25 January 2023

Fig. 1. Two Intel Aero Ready To Fly quadrotors flying.

of more elaborate control laws. It is commonly studied under the use of gradient control laws, which are defined using artificial potential fields. For single integrator modeled agents, it has been studied by Krick et al. (2008) and V. Dimarogonas and Johansson (2008), and for double integrator modeled agents by Oh and Ahn (2014). An example of a different approach is the bearing-based formation control, described for example in the works by Zhao and Zelazo (2017), Ahn (2020) and Tang et al. (2021).

In this work, it is assumed that the vehicles have access to measurements of their orientation, and therefore, a displacement-based approach is considered, in which consensus protocols are typically used to achieve coordination between the vehicles in a distributed manner. The consensus problem, as the name entails, consists of driving a group of agents, over a network, to an agreement on some value, considering that only local information is exchanged or perceived. A body of work has been dedicated to the displacement-based approach, following the groundbreaking results presented in the works by Fax and Murray (2004), Ren et al. (2004), Olfati-Saber and Murray (2004) and Ren and Atkins (2007). The work by Ren et al. (2004) is an example of this approach applied to vehicles modeled as single integrators. However, a wide variety of vehicles are modeled with second- or higher-order models. For that reason, consensus protocols for agents modeled by multiple integrators have been proposed in the literature. Second-order algorithms are well studied and can be applied, for example, to vehicles actuated on acceleration. These were proposed and analyzed, for example, by Ren and Atkins (2007), and later addressed with further detail by both Zhu et al. (2009) and Yu et al. (2010). The work by Ren and Atkins (2007) analyzes the convergence of a second-order consensus protocol and introduces a sufficient condition for consensus, given by a graphical condition and a conservative bound on a coupling gain. A non-conservative bound is later introduced by both Zhu et al. (2009) (which studies a general form second-order consensus algorithm) and Yu et al. (2010) (which also focuses on determining an upper bound on the input delay for which consensus is achieved), achieving a necessary and sufficient condition for consensus.

Several developments, such as the works by Ren et al. (2006), Ren et al. (2007), Mukherjee and Zelazo (2019) and Tegling et al. (2019), also approached higher-order protocols. In one of these works (Ren et al., 2007), the authors introduced a protocol for higher-order agent dynamics and claim that there exists a set of coupling gains for the proposed consensus protocol that leads to convergence, but make no further description on how these parameters influence the convergence. It was only more recently that some works, such as the ones by Cao and Sun (2014) and Huang et al. (2018), focused on third-order algorithms specifically. The work by Cao and Sun (2014) studies third-order consensus for the case of undirected graphs. More recently, Huang et al. (2018) consider directed graphs, and attempt to extend the second-order results presented by Yu et al. (2010) to triple integrator agents, but do not provide exact bounds on the coupling gains that lead to consensus.

Considering the importance of developing robust control algorithms for the coordinated motion of multiple unmanned autonomous vehicles, this work seeks to develop distributed control algorithms for formation tracking, and validate the devised solutions by exemplifying their application to multirotor vehicles (see Fig. 1). Vehicles are complex systems, and their dynamical models are subject to errors and parameter uncertainties that can be perceived as disturbances to the nominal system that is being considered. When vehicles are modeled as double integrators, a third-order consensus protocol, in contrast with a traditional second-order protocol, enables the use of integral action in the formation controller, which enhances the system with the ability to reject constant disturbances. This can be of paramount importance in some scenarios, and is particularly useful for multirotor vehicles. For this reason, a third-order consensus protocol is considered in this work. Nonetheless, to overcome the gaps in the literature that is provided, for example, in the works by Cao and Sun (2014) and Huang et al. (2018), the third-order consensus protocol must be analyzed further. Namely, it is necessary to deepen the analysis regarding robustness and convergence conditions.

This paper presents an analysis of a third-order consensus protocol, providing necessary and sufficient conditions for convergence by determining the exact bounds on the coupling gains that lead the group of agents to consensus. These bounds provide novel criteria for the third-order consensus protocol and turn out to be a generalization of the ones described in the literature for second-order consensus, in the sense that the latter can be recovered as a special case. The effect of disturbances on the overall convergence of the system is also evaluated, with special focus on constant disturbances. The results are applied to the formation control problem in order to introduce integral action in the controller for vehicles modeled as double integrators. To conclude the analysis, the inclusion of goal seeking terms is studied.

Abbreviated statements, without proofs, of some of the results detailed in this paper were previously presented by the authors (Trindade et al., 2020). This paper includes the proofs that were previously omitted, furthers the analysis concerning robustness in the presence of bounded disturbances and constant disturbances, and enhances the results concerning goal seeking terms.

The remainder of this paper is organized as follows. Section 2 presents the relevant notation, as well as some concepts of graph theory, important in the context of this paper. The problem statement is given in Section 3 and then, in Section 4, the consensus protocols of interest are introduced, followed by a convergence analysis and some illustrative examples. Section 5 details the application of the previously introduced consensus protocols in the development of the formation tracking controller, also followed by an example that illustrates these results. Section 6 describes the application of the proposed algorithms to multirotor vehicles for experimental validation and presents the results. Finally, concluding remarks are provided in Section 7.

2. Preliminaries

2.1. Notation

The notation used throughout this paper is introduced here. Vectors are set in lower case bold and matrices in upper case bold. The set of real numbers is denoted by $\mathbb{R}$, the subset of positive real numbers is denoted by $\mathbb{R}^+$, and the set of real numbers except zero, i.e. $\mathbb{R} \setminus \{0\}$, is denoted by $\mathbb{R}_{\neq 0}$. The set of complex numbers is denoted by $\mathbb{C}$, and for a complex number $z \in \mathbb{C}$, $\mathrm{Re}(z)$ denotes its real part and $\mathrm{Im}(z)$ denotes its imaginary part. The m-dimensional Euclidean space is denoted by $\mathbb{R}^m$, and $\|\mathbf{x}\|_p$ denotes the l_p-norm of a vector $\mathbf{x} \in \mathbb{R}^m$. For $p = 2$ (the Euclidean norm) only $\|\mathbf{x}\|$ is used. The dot notation is used to define the time derivative (as in $\dot{\mathbf{x}}$), and the number of dots its order (e.g. $\ddot{\mathbf{x}}$ denotes the second time derivative). The $n \times n$ identity matrix is denoted by $\mathbf{I}_n$, and $\mathbf{0}_{n\times m}$ denotes an $n \times m$ matrix of zeros (when it is possible to infer on the dimensions, only $\mathbf{0}$ is used). Also, $\mathbf{1}_n$ denotes the $n \times 1$ vector of ones, $\bar{x} = \mathbf{1}_n^\top \mathbf{x}/n$ denotes the average of the entries of a vector $\mathbf{x} \in \mathbb{R}^n$, and $\mathbf{e}_i \in \mathbb{R}^n$ is the vector with one in the ith component and zeros elsewhere. Finally, the symbol $\otimes$ denotes the Kronecker product.

2.2. Graph theory

When working with multi-agent systems, the communication network is typically described using graph theory.

Definition 1. A directed graph $\mathcal{G}$, usually abbreviated to digraph, consists of a pair of sets $(\mathcal{V}, \mathcal{A})$, where $\mathcal{V}$ is a non-empty finite set of vertices, and $\mathcal{A} \in \mathcal{V}^2$ is a finite set of ordered pairs of vertices, called arcs.

An excellent and self-contained exposition on the theory of digraphs considered in this work is provided by Veerman and Lyons (2020). Some of the notation and terminology used here is borrowed from that work. There, the authors consider undirected graphs as a specific case of digraphs, where the main difference is that, in the case of undirected graphs, arcs are unordered pairs of vertices. For that reason, definitions are provided for digraphs only.

An arc, connecting a vertex i to j, will be denoted by $i \to j$. Informally, for an arc $i \to j$, one says that i sends information to j, or that j "sees" i. A digraph is said to be simple if it does not contain self-loops (vertices that see themselves). The set $\mathcal{N}_i \subseteq \mathcal{V}$ of vertices seen by i (excluding itself) is called the neighborhood of i, and $\mathcal{V}_S \subseteq \mathcal{V}$ is the set of vertices that see themselves (have a self-loop). If a digraph is weighted, the weight associated to an arc $i \to j$ is denoted by $k_{j\leftarrow i} \in \mathbb{R}$. When there is an arc $i \to j$, then $k_{j\leftarrow i} > 0$, and when there is no arc, $k_{j\leftarrow i} = 0$. These weights can be used to describe, for example, the strength of the interactions between agents, or their capability to exchange information. If the digraph is not weighted, then all weights associated to arcs in the digraph are considered to be one.

Definition 2. A directed path is an ordered sequence of arcs, connecting two distinct vertices in the digraph. Then:

(i) A digraph has a spanning tree when there is at least one vertex that has a directed path to all others.

(ii) A digraph is strongly connected when for any pair of vertices there is a directed path from one vertex to the other.

Definition 3. Consider a digraph $\mathcal{G}$ with n vertices. Then:

(i) The (directed) Laplacian matrix $\mathbf{L} = \left[l_{ij}\right] \in \mathbb{R}^{n\times n}$ is defined as $l_{ij} = -k_{i\leftarrow j}$ for $i \neq j$, and $l_{ii} = -\sum_{j\neq i} l_{ij}$.

(ii) The generalized Laplacian matrix $\boldsymbol{\mathcal{L}}$ is defined as $\boldsymbol{\mathcal{L}} = \mathbf{L} + \mathbf{S}$, where $\mathbf{S} = \sum_{i\in\mathcal{V}_S} k_{i\leftarrow i}\mathbf{e}_i\mathbf{e}_i^\top$ is a diagonal matrix of self-loop weights.

The Laplacian matrix has some relevant properties, such as null row sum, meaning it has at least one null eigenvalue with eigenvector $\mathbf{1}_n$. The following results present some relevant properties of both the Laplacian and the generalized Laplacian matrices.

Lemma 1 (Ren et al., 2004). *The Laplacian* $\mathbf{L}$ *of a digraph* $\mathcal{G}$ *has a single null eigenvalue and all other eigenvalues have positive real part if and only if the digraph has a spanning tree.*

Proposition 1. *All eigenvalues of the generalized Laplacian* $\boldsymbol{\mathcal{L}}$ *of a digraph* $\mathcal{G} = (\mathcal{V}, \mathcal{A})$ *that has a spanning tree have positive real part if and only if one of the vertices with a directed path to all others has a self-loop.*

Proof. The proof is presented in the Appendix B. □

3. Problem statement

The problem at hand consists in the development of a distributed and cooperative control algorithm to enable a team of n vehicles to track a time-varying formation and converge to their desired position in space. It is assumed that the desired position for each vehicle i is given as a function of time, i.e., a trajectory $\mathbf{p}_i^{\mathbf{d}}(t) \in \mathbb{R}^3$ is defined for all $t > 0$, with known and continuous first and second time derivatives.

As previously stated, dynamical models for vehicles are subject to errors and parameter uncertainties that can be perceived as disturbances to the nominal system that is being considered. It is with that in mind that each vehicle is modeled by

$$\begin{cases} \dot{\mathbf{p}}_i = \mathbf{v}_i \\ \dot{\mathbf{v}}_i = \mathbf{u}_i + \mathbf{d}_i \end{cases}, \tag{1}$$

where $\mathbf{p}_i, \mathbf{v}_i \in \mathbb{R}^3$ denote the position and velocity of the ith vehicle, respectively, $\mathbf{u}_i \in \mathbb{R}^3$ is the control input of the vehicle, in this case, its acceleration, and $\mathbf{d}_i \in \mathbb{R}^3$ is an unknown disturbance acting on the ith vehicle.

Let $\mathbf{p}_{ij} := (\mathbf{p}_i - \mathbf{p}_j)$ and $\mathbf{p}_{ij}^{\mathbf{d}} := (\mathbf{p}_i^{\mathbf{d}} - \mathbf{p}_j^{\mathbf{d}})$ denote the relative position and the desired relative position of vehicle i with respect to vehicle j, respectively. In order to track a prescribed formation, the goal is to have $\mathbf{p}_{ij}(t) - \mathbf{p}_{ij}^{\mathbf{d}}(t) \to \mathbf{0}$ as $t \to \infty$. The vehicles should also seek to asymptotically reach their desired position in space, i.e., to have $\mathbf{p}_i(t) - \mathbf{p}_i^{\mathbf{d}}(t) \to \mathbf{0}$ as $t \to \infty$. However, each vehicle is considered to have limited information about the complete system. More specifically, it is assumed that each vehicle has access to the relative position and velocity of some of the other vehicles (its neighbors), and only a limited set of vehicles has information about its own position and velocity.

4. Consensus protocols

Here, consensus protocols used for distributed coordination of multiple agents, communicating over a network described by a digraph $\mathcal{G} = (\mathcal{V}, \mathcal{A})$, are introduced. Firstly, consensus protocols for agents with single and double integrator dynamics, previously described in the literature, are presented. Then, a consensus protocol for agents with triple integrator dynamics is introduced, followed by an analysis of its convergence properties.

4.1. Single and double integrator dynamics

Consider a group of n agents, each described by the single integrator dynamics

$$\dot{\beta}_i = \mu_i, \tag{2}$$

with $\beta_i, \mu_i \in \mathbb{R}$, where μ_i is the control input of the agent. Recall that if $j \notin \mathcal{N}_i$ (i.e., j is not seen by i), then by definition, $k_{i\leftarrow j} = 0$. The consensus protocol for this system is given by

$$\mu_i = -\sum_{j\in\mathcal{N}_i} k_{i\leftarrow j}\left(\beta_i - \beta_j\right) = -\sum_{j\neq i} k_{i\leftarrow j}\left(\beta_i - \beta_j\right). \tag{3}$$

The goal of protocol (3) is to guarantee that consensus is achieved, i.e., $|\beta_i - \beta_j| \to 0$ as $t \to \infty$. Note that each agent i only needs to know the difference between its state and the state of its neighbors, $(\beta_i - \beta_j)$, and does not need to know its absolute state. Moreover, note that (3) can be written in vector form using the Laplacian $\mathbf{L}$ of the digraph $\mathcal{G}$, as $\boldsymbol{\mu} = -\mathbf{L}\boldsymbol{\beta}$, where $\boldsymbol{\beta} = \left[\beta_1 \ \cdots \ \beta_n\right]^\top \in \mathbb{R}^n$ and $\boldsymbol{\mu} = \left[\mu_1 \ \cdots \ \mu_n\right]^\top \in \mathbb{R}^n$. Therefore, the feedback actuated system becomes $\dot{\boldsymbol{\beta}} = -\mathbf{L}\boldsymbol{\beta}$. As shown, for example, by Ren et al. (2004), the existence of a spanning tree on the digraph which describes the interaction topology is a necessary and sufficient condition for achieving consensus when agents are modeled as single integrators.

Consider now a group of n agents modeled as double integrators, i.e.,

$$\begin{cases} \dot{\alpha}_i = \beta_i \\ \dot{\beta}_i = \mu_i \end{cases}, \tag{4}$$

with $\alpha_i, \beta_i, \mu_i \in \mathbb{R}$, where μ_i is the control input of the ith agent. For this system, the consensus protocol

$$\mu_i = -\sum_{j\in\mathcal{N}_i} k_{i\leftarrow j}\left[\gamma\left(\beta_i - \beta_j\right) + \left(\alpha_i - \alpha_j\right)\right], \tag{5}$$

where $\gamma \in \mathbb{R}^+$ is a coupling gain, was proposed, for example, in the work by Ren and Atkins (2007). The goal of protocol (5) is to achieve consensus, i.e., $|\alpha_i - \alpha_j| \to 0$ and $|\beta_i - \beta_j| \to 0$ as $t \to \infty$. Note that (5) can be written in vector form as $\boldsymbol{\mu} = -\gamma \mathbf{L}\boldsymbol{\beta} - \mathbf{L}\boldsymbol{\alpha}$, where $\boldsymbol{\alpha} = \begin{bmatrix}\alpha_1 & \cdots & \alpha_n\end{bmatrix}^\top \in \mathbb{R}^n$, $\boldsymbol{\beta} = \begin{bmatrix}\beta_1 & \cdots & \beta_n\end{bmatrix}^\top \in \mathbb{R}^n$, and $\boldsymbol{\mu} = \begin{bmatrix}\mu_1 & \cdots & \mu_n\end{bmatrix}^\top \in \mathbb{R}^n$. Thus, the feedback actuated system can be written as

$$\begin{bmatrix}\dot{\boldsymbol{\alpha}} \\ \dot{\boldsymbol{\beta}}\end{bmatrix} = \mathbf{G}(\mathbf{L}) \begin{bmatrix}\boldsymbol{\alpha} \\ \boldsymbol{\beta}\end{bmatrix}, \tag{6}$$

with $\mathbf{G} : \mathbb{R}^{k\times k} \to \mathbb{R}^{2k\times 2k}$, where

$$\mathbf{G}(\mathbf{K}) := \begin{bmatrix}\mathbf{0} & \mathbf{I}_k \\ -\mathbf{K} & -\gamma\mathbf{K}\end{bmatrix}.$$

Ren and Atkins (2007) have shown that, unlike the single integrator case, the existence of a spanning tree is not a sufficient condition for reaching consensus. The same work then introduces a sufficient condition in the form of a conservative bound on the coupling gain γ of protocol (5). Later, the work by Yu et al. (2010) provides an exact bound on γ that guarantees that the agents reach consensus, which is reproduced here for completeness.

Proposition 2 (*Yu et al., 2010*). *The protocol (5) reaches consensus asymptotically if and only if the digraph which describes the interaction topology of the agents has a spanning tree and*

$$\gamma^2 > \max_{\eta_i \neq 0} \frac{\mathrm{Im}(\eta_i)^2}{\mathrm{Re}(\eta_i)\left(\mathrm{Re}(\eta_i)^2 + \mathrm{Im}(\eta_i)^2\right)}$$

where η_i represents the ith eigenvalue of $\mathbf{L}$.

4.2. Triple integrator dynamics

Consider now that each agent is described by

$$\begin{cases}\dot{\theta}_i = \alpha_i \\ \dot{\alpha}_i = \beta_i \\ \dot{\beta}_i = \mu_i\end{cases}, \tag{7}$$

with $\theta_i, \alpha_i, \beta_i, \mu_i \in \mathbb{R}$, where μ_i is the control input of the ith agent. For this system, consider the consensus protocol

$$\mu_i = -\sum_{j\in\mathcal{N}_i} k_{i\leftarrow j}\left[\gamma\left(\beta_i - \beta_j\right) + \left(\alpha_i - \alpha_j\right) + \zeta\left(\theta_i - \theta_j\right)\right], \tag{8}$$

where $\gamma \in \mathbb{R}_{\neq 0}$ and $\zeta \in \mathbb{R}_{\neq 0}$ are coupling gains. Note that no assumptions are made on the sign of γ or ζ, as convergence conditions will be derived later on. In order to achieve consensus, the goal is to have $|\theta_i - \theta_j| \to 0$, $|\alpha_i - \alpha_j| \to 0$, and $|\beta_i - \beta_j| \to 0$ as $t \to \infty$. Note that, in vector form, (8) can be written as

$$\boldsymbol{\mu} = -\gamma\mathbf{L}\boldsymbol{\beta} - \mathbf{L}\boldsymbol{\alpha} - \zeta\mathbf{L}\boldsymbol{\theta}, \tag{9}$$

with $\boldsymbol{\theta} = \begin{bmatrix}\theta_1 & \cdots & \theta_n\end{bmatrix}^\top \in \mathbb{R}^n$, $\boldsymbol{\alpha} = \begin{bmatrix}\alpha_1 & \cdots & \alpha_n\end{bmatrix}^\top \in \mathbb{R}^n$, $\boldsymbol{\beta} = \begin{bmatrix}\beta_1 & \cdots & \beta_n\end{bmatrix}^\top \in \mathbb{R}^n$, and $\boldsymbol{\mu} = \begin{bmatrix}\mu_1 & \cdots & \mu_n\end{bmatrix}^\top \in \mathbb{R}^n$. Therefore, for the third-order dynamics, the feedback actuated system can be written as

$$\dot{\mathbf{x}} = \mathbf{H}(\mathbf{L})\mathbf{x} \tag{10}$$

with $\mathbf{x} := \begin{bmatrix}\boldsymbol{\theta}^\top & \boldsymbol{\alpha}^\top & \boldsymbol{\beta}^\top\end{bmatrix}^\top$ and $\mathbf{H} : \mathbb{R}^{k\times k} \to \mathbb{R}^{3k\times 3k}$, where

$$\mathbf{H}(\mathbf{K}) := \begin{bmatrix}\mathbf{0} & \mathbf{I}_k & \mathbf{0} \\ \mathbf{0} & \mathbf{0} & \mathbf{I}_k \\ -\zeta\mathbf{K} & -\mathbf{K} & -\gamma\mathbf{K}\end{bmatrix},$$

or, in compact form,

$$\dddot{\boldsymbol{\theta}}(t) = -\mathbf{L}\left(\gamma\ddot{\boldsymbol{\theta}}(t) + \dot{\boldsymbol{\theta}}(t) + \zeta\boldsymbol{\theta}(t)\right).$$

Remark 1. In the protocol (8), as well as in the protocol (5), there is no coupling gain for α_i. This introduces no loss of generality, since the effect of such a gain can be encapsulated in the digraph by scaling the weights $k_{i\leftarrow j}$ and then adjusting γ and ζ accordingly. More concretely, consider that, in contrast with (9), one writes

$$\boldsymbol{\mu} = -\gamma\mathbf{L}\boldsymbol{\beta} - \rho\mathbf{L}\boldsymbol{\alpha} - \zeta\mathbf{L}\boldsymbol{\theta},$$

where $\rho \in \mathbb{R}^+$ would be a coupling parameter for α_i. Defining $\tilde{\mathbf{L}} := \rho\mathbf{L}$, $\tilde{\gamma} := \gamma/\rho$ and $\tilde{\zeta} := \zeta/\rho$, this becomes

$$\boldsymbol{\mu} = -\tilde{\gamma}\tilde{\mathbf{L}}\boldsymbol{\beta} - \tilde{\mathbf{L}}\boldsymbol{\alpha} - \tilde{\zeta}\tilde{\mathbf{L}}\boldsymbol{\theta},$$

and the shape of (9) is recovered. Note that $\tilde{\mathbf{L}}$ is associated with the same digraph as $\mathbf{L}$, with the weights $k_{i\leftarrow j}$ scaled by the factor ρ.

4.3. Convergence analysis

Now that the relevant consensus protocols have been introduced, focus is turned to the analysis of the stability properties of the proposed third-order consensus protocol (8) and its ability to achieve consensus. To do so, some concepts are first introduced. Let $\mathbf{J}$ be the real Jordan form of $\mathbf{L}$, such that $\mathbf{L} = \mathbf{V}\mathbf{J}\mathbf{V}^{-1}$. Note that $\mathbf{L}$ has at least a null eigenvalue associated with the eigenvector $\mathbf{1}_n$ and, according to Veerman and Lyons (2020), the algebraic and geometric multiplicities of the null eigenvalues are equal. Therefore, and without loss of generality, $\mathbf{J}$ and $\mathbf{V}$ can be written as

$$\mathbf{J} = \begin{bmatrix}0 & \mathbf{0} \\ \mathbf{0} & \mathbf{J}^*\end{bmatrix} \quad \text{and} \quad \mathbf{V} = \begin{bmatrix}\mathbf{v}_1 & \cdots & \mathbf{v}_n\end{bmatrix},$$

where $\mathbf{J}^* \in \mathbb{R}^{(n-1)\times(n-1)}$ and $\mathbf{v}_k \in \mathbb{R}^n$, $k = 1, \ldots, n$, with $\mathbf{v}_1 = \mathbf{1}_n$. Also, let $\mathbf{V}^{-1} = \begin{bmatrix}\mathbf{w}_1 & \cdots & \mathbf{w}_n\end{bmatrix}^\top$, where $\mathbf{w}_k \in \mathbb{R}^n$, $k = 1, \ldots, n$. Let $\mathbf{w}_1 = \mathbf{r}$ and note that, since $\mathbf{V}^{-1}\mathbf{V} = \mathbf{I}_n$, then $\mathbf{r}^\top\mathbf{1}_n = 1$, and $\mathbf{w}_k^\top\mathbf{1}_n = 0$, $k = 2, \ldots, n$. Furthermore, $\mathbf{r}$ is known to be a non-negative vector (i.e., all its entries are non-negative).

Proposition 3. *Consider the map* $\mathbf{H}$ *defined previously, with* $\gamma, \zeta \in \mathbb{R}$. *The pair* $(\lambda, \mathbf{v})$ *is an eigenpair of* $\mathbf{H}(\mathbf{K})$ *if and only if* $\mathbf{v} = \begin{bmatrix}\mathbf{u}^\top & \lambda\mathbf{u}^\top & \lambda^2\mathbf{u}^\top\end{bmatrix}^\top$ *and* λ *is a root of* $\lambda^3 + (\gamma\lambda^2 + \lambda + \zeta)\eta = 0$, *where* $(\eta, \mathbf{u})$ *is an eigenpair of* $\mathbf{K}$.

Proof. Considering $\mathbf{v} = \begin{bmatrix}\mathbf{v}_1^\top & \mathbf{v}_2^\top & \mathbf{v}_3^\top\end{bmatrix}^\top$, it holds that

$$\lambda\mathbf{v} = \mathbf{H}(\mathbf{K})\mathbf{v} \Leftrightarrow \begin{cases}\lambda\mathbf{v}_1 = \mathbf{v}_2 & \text{(a)} \\ \lambda\mathbf{v}_2 = \mathbf{v}_3 & \text{(b)} \\ \lambda\mathbf{v}_3 = -\zeta\mathbf{K}\mathbf{v}_1 - \mathbf{K}\mathbf{v}_2 - \gamma\mathbf{K}\mathbf{v}_3 & \text{(c)}\end{cases}. \tag{11}$$

Applying the first equation to the second yields $\mathbf{v}_3 = \lambda^2\mathbf{v}_1$. Applying this, together with (11a), to (11c) yields

$$\lambda^3\mathbf{v}_1 = -\left(\zeta + \lambda + \gamma\lambda^2\right)\mathbf{K}\mathbf{v}_1.$$

It follows that $\mathbf{v}_1$ is an eigenvector of $\mathbf{K}$. Choosing $\mathbf{v}_1 = \mathbf{u}$ such that $\mathbf{K}\mathbf{u} = \eta\mathbf{u}$, one finally obtains $\lambda^3 = -(\zeta + \lambda + \gamma\lambda^2)\eta$, which concludes the proof. □

Considering the result introduced in Proposition 3, the eigenvalues of $\mathbf{H}(\mathbf{L})$ can now be related with the eigenvalues of $\mathbf{L}$. More concretely, if $\eta_i \in \mathbb{C}$, $i = 1, \ldots, n$ are the eigenvalues of $\mathbf{L}$, then the roots λ_{ij}, $j = 1, 2, 3$, of $h_i(\lambda) = 0$ with

$$h_i(\lambda) := \lambda^3 + (\gamma\lambda^2 + \lambda + \zeta)\eta_i,$$

are the three eigenvalues of $\mathbf{H}(\mathbf{L})$ associated to η_i. It is straightforward to conclude that $\eta_i = 0$ implies that $\lambda_{i1} = \lambda_{i2} = \lambda_{i3} = 0$, i.e., for each null eigenvalue in $\mathbf{L}$ there are three null eigenvalues in $\mathbf{H}(\mathbf{L})$. Moreover, since by definition $\zeta \neq 0$, it is possible to conclude that $\lambda = 0$ is a root of $h_i(\lambda)$ only if $\eta_i = 0$. Therefore $\mathbf{H}(\mathbf{L})$ has exactly three null eigenvalues for each null eigenvalue of $\mathbf{L}$.

Consider the Lyapunov transformation described by

$$\begin{cases}\boldsymbol{\theta}^* = \mathbf{V}^{-1}\boldsymbol{\theta} := \begin{bmatrix}\theta_1^* & \cdots & \theta_n^*\end{bmatrix}^\top \\ \boldsymbol{\alpha}^* = \mathbf{V}^{-1}\boldsymbol{\alpha} := \begin{bmatrix}\alpha_1^* & \ldots & \alpha_n^*\end{bmatrix}^\top \\ \boldsymbol{\beta}^* = \mathbf{V}^{-1}\boldsymbol{\beta} := \begin{bmatrix}\beta_1^* & \cdots & \beta_n^*\end{bmatrix}^\top\end{cases}. \tag{12}$$

Now, note that

$$\boldsymbol{\theta} = \mathbf{V}\boldsymbol{\theta}^* = \theta_1^*\mathbf{1}_n + \theta_2^*\mathbf{v}_2 + \cdots + \theta_n^*\mathbf{v}_n. \tag{13}$$

Furthermore, note that $\mathbf{v}_k$, $k = 1, \ldots, n$, are linearly independent vectors ($\mathbf{V}$ is invertible). To reach consensus one must have $\boldsymbol{\theta} \to \mathbf{1}_n\theta_c(t)$. Therefore, it is possible to conclude that $\theta_c(t) = \theta_1^*(t)$ and consensus is reached if and only if $\boldsymbol{\theta}_{2,n}^* \to \mathbf{0}$, with $\boldsymbol{\theta}_{2,n}^* := \begin{bmatrix}\theta_2^* & \cdots & \theta_n^*\end{bmatrix}^\top$. Bear in mind that $\theta_1^*(t)$ corresponds to the consensus value and $\boldsymbol{\theta}_{2,n}^*$ can be regarded as a transformed consensus error.

Conditions on the eigenvalues of $\mathbf{H}(\mathbf{L})$ that allow for achieving consensus are now presented. A similar version of the result that follows was stated by Ren et al. (2007). Nonetheless, a proof is hereby presented for the sake of completeness. It is worth noting that it is straightforward to extend this result to any number of integrators.

Lemma 2. *Consider the consensus protocol (8) for agents modeled by triple integrator dynamics (7). Consensus is achieved if and only if the matrix $\mathbf{H}(\mathbf{L})$ has exactly three null eigenvalues and the remaining eigenvalues have negative real part. More concretely, when reaching consensus (for large t),*

$$\boldsymbol{\theta}(t) \to \mathbf{1}_n\mathbf{r}^\top\left(\boldsymbol{\theta}(0) + \boldsymbol{\alpha}(0)t + \boldsymbol{\beta}(0)\frac{t^2}{2}\right), \tag{14}$$

where $\mathbf{r}$ is the non-negative eigenvector of $\mathbf{L}^\top$ associated to the null eigenvalue, such that $\mathbf{1}_n^\top\mathbf{r} = 1$.

Proof. The third-order integrator dynamics (7) actuated by the consensus protocol (8) are given by (10). Considering the previously mentioned Lyapunov transformation, the new system dynamics are given by

$$\begin{cases}\dot{\boldsymbol{\theta}}^* = \boldsymbol{\alpha}^* \\ \dot{\boldsymbol{\alpha}}^* = \boldsymbol{\beta}^* \\ \dot{\boldsymbol{\beta}}^* = -\mathbf{J}\boldsymbol{\alpha}^* - \gamma\mathbf{J}\boldsymbol{\beta}^* - \zeta\mathbf{J}\boldsymbol{\theta}^*\end{cases}.$$

Now, consider the equivalent system description

$$\begin{cases}\dddot{\theta}_1^* = 0 & \text{(a)} \\ \dddot{\boldsymbol{\theta}}_{2,n}^* = -\mathbf{J}^*\left(\gamma\ddot{\boldsymbol{\theta}}_{2,n}^* + \dot{\boldsymbol{\theta}}_{2,n}^* + \zeta\boldsymbol{\theta}_{2,n}^*\right) & \text{(b)}\end{cases}. \tag{15}$$

Recall that consensus is reached when $\boldsymbol{\theta}_{2,n}^* \to \mathbf{0}$. The solution of (15a) gives

$$\theta_1^*(t) = \theta_1^*(0) + \alpha_1^*(0)t + \beta_1^*(0)\frac{t^2}{2!}.$$

There are three null eigenvalues associated with the subsystem (15a). To have $\boldsymbol{\theta}_{2,n}^* \to \mathbf{0}$, then the remaining eigenvalues of $\mathbf{H}(\mathbf{L})$ must have negative real part. To show that (14) holds, note that when $\boldsymbol{\theta}_{2,n}^* \to \mathbf{0}$, it follows that $\boldsymbol{\theta} \to \mathbf{1}_n\theta_1^*(t)$, and noting that $\theta_1^* = \mathbf{r}^\top\boldsymbol{\theta}$, $\alpha_1^* = \mathbf{r}^\top\boldsymbol{\alpha}$, and $\beta_1^* = \mathbf{r}^\top\boldsymbol{\beta}$,

$$\theta_1^*(t) = \mathbf{r}^\top\left(\boldsymbol{\theta}(0) + \boldsymbol{\alpha}(0)t + \boldsymbol{\beta}(0)\frac{t^2}{2!}\right).$$

The consensus values for $\boldsymbol{\alpha}$ and $\boldsymbol{\beta}$ can be obtained by taking the time derivative. □

The result introduced in Lemma 2 provides conditions on the eigenvalues of $\mathbf{H}(\mathbf{L})$ for which the agents achieve consensus. This result will now be used to obtain bounds on the coupling gains γ and ζ of the protocol (8) that guarantee the agents converge to a consensus. More specifically, exact bounds on the coupling gains are obtained, leading to necessary and sufficient conditions for convergence.

Although not widely known, probably due to a lack of applications, the extension of the Routh–Hurwitz criterion to polynomials with complex coefficients has been around for several years now (Frank, 1946). This extended criterion is explored here to determine conditions for convergence of the third-order consensus protocol.

Lemma 3 (Frank, 1946). *A third degree polynomial with complex coefficients, of the form*

$$p(\lambda) = \lambda^3 + (a_2 + b_2 j)\lambda^2 + (a_1 + b_1 j)\lambda + (a_0 + b_0 j),$$

with $a_i, b_i \in \mathbb{R}$, $i = 0, 1, 2$, has all roots with negative real part if and only if $a_2 > 0$,

$$\begin{vmatrix} a_2 & a_0 & -b_1 \\ 1 & a_1 & -b_2 \\ 0 & b_1 & a_2 \end{vmatrix} > 0, \quad \text{and} \quad \begin{vmatrix} a_2 & a_0 & 0 & -b_1 & 0 \\ 1 & a_1 & 0 & -b_2 & -b_0 \\ 0 & a_2 & a_0 & 0 & -b_1 \\ 0 & b_1 & 0 & a_2 & a_0 \\ 0 & b_2 & b_0 & 1 & a_1 \end{vmatrix} > 0.$$

The following result follows from Lemma 3 and will be essential in proving the main result of the paper.

Lemma 4. *A third-degree polynomial with complex coefficients, of the form*

$$p_3(\lambda) = \lambda^3 + \eta\left(\gamma\lambda^2 + \lambda + \zeta\right),$$

where $\gamma, \zeta \in \mathbb{R}$ and $\eta \in \mathbb{C}$, with $\mathrm{Re}(\eta) > 0$, has all its roots in the open left half-plane if and only if

$$\begin{cases}\gamma > \sqrt{\frac{1-\xi^2}{\xi\omega_n}} \\ 0 < \zeta < \left[\frac{\omega_n}{\xi}\left(\gamma - \sqrt{\frac{1-\xi^2}{\xi\omega_n}}\right)\right]\end{cases},$$

where $\omega_n = |\eta|$ and $\xi = \mathrm{Re}(\eta)/\omega_n$.

Proof. The proof is presented in the Appendix C. □

The following theorem is the main result of the paper.

Theorem 1. *The consensus protocol (8) for triple integrator agents achieves consensus asymptotically if and only if the digraph which describes the interaction topology of the agents has a spanning tree and*

$$\begin{cases}\gamma > \max_{\eta_i \neq 0}\sqrt{\frac{1-\xi_i^2}{\xi_i\omega_{n_i}}} & \text{(a)} \\ 0 < \zeta < \min_{\eta_i \neq 0}\left[\frac{\omega_{n_i}}{\xi_i}\left(\gamma - \sqrt{\frac{1-\xi_i^2}{\xi_i\omega_{n_i}}}\right)\right] & \text{(b)}\end{cases}, \tag{16}$$

where $\omega_{n_i} = |\eta_i|$ and $\xi_i = \mathrm{Re}(\eta_i)/\omega_{n_i}$ represent the natural frequency and damping coefficient, respectively, associated with the ith eigenvalue of $\mathbf{L}$.

Proof. From Lemma 2, the protocol (8) achieves consensus when $\mathbf{H}(\mathbf{L})$ has exactly three null eigenvalues and the remaining eigenvalues have negative real part. But $\mathbf{H}(\mathbf{L})$ has exactly three null eigenvalues if and only if $\mathbf{L}$ has exactly one null eigenvalue. Thus, it follows from Lemma 1 that there must exist a spanning tree in the associated digraph. Without loss of generality, let $\eta_1 = 0$ and $\eta_i \in \mathbb{C}$, $i = 2, \ldots, n$, be the eigenvalues of $\mathbf{L}$. Also from Lemma 1, it is known that $\mathrm{Re}(\eta_i) > 0$ for $i = 2, \ldots, n$. Therefore, the result presented in Lemma 4 can be applied to the third degree polynomial $h_i(\lambda)$ associated to an eigenvalue η_i of $\mathbf{L}$. Finally, noting that all the roots of $h_i(\lambda)$ associated with the non-null eigenvalues η_i of $\mathbf{L}$ must have negative real part, the conditions that must be met are (16) and the proof is concluded. □

Remark 2. Note that it is straightforward to choose γ and ζ that satisfy the conditions (16) presented in Theorem 1. Since (16a) only concerns γ, one can start by picking γ to satisfy that lower bound (that is always possible since the lower bound is a non-negative real number). Then one can choose ζ that satisfies (16b), with γ fixed. If γ satisfies (16a), then the upper bound on ζ is positive and the set of possible values for ζ, defined by (16b), is non-empty.

There are some particular cases of interest, in which all the eigenvalues of $\mathbf{L}$ are real. This is the case when, for example, the graph is undirected. When the interaction topology follows a leader–follower structure, all eigenvalues of $\mathbf{L}$ are also real (Fax & Murray, 2004).

Corollary 1. *If the non-null eigenvalues of* $\mathbf{L}$ *are real, then the third-order consensus protocol (8) achieves consensus asymptotically if and only if the digraph associated to the interaction topology has a spanning tree and*

$$\begin{cases} \gamma > 0 & \text{(a)} \\ 0 < \zeta < \min_{\eta_i \neq 0} \left(\gamma \eta_i\right) & \text{(b)} \end{cases} \tag{17}$$

where η_i, $i = 1, \dots, n$ *represents the ith eigenvalue of* $\mathbf{L}$.

Proof. When the non-null eigenvalues of $\mathbf{L}$ are real, by definition, $\omega_{n_i} = |\eta_i| = \eta_i$ and $\xi_i = \mathrm{Re}\left(\eta_i\right)/\omega_{n_i} = \frac{\eta_i}{\eta_i} = 1$. Simple substitution in the conditions presented in Theorem 1 yields the conditions for this particular case. □

Remark 3. Note that the result described in Proposition 2 regarding the consensus protocol (5), and presented by Yu et al. (2010), can also be obtained from Theorem 1 as a particular case. In fact, when ζ is set to zero, the consensus protocol (8) degenerates into the protocol (5) acting on the third-order integrator dynamics (7) and θ becomes a pure integrator. As a result, one has $h_i(\lambda) = \lambda g_i(\lambda)$, where $g_i(\lambda) := \lambda^2 + \gamma\eta_i\lambda + \eta_i$ plays the role of $h_i(\lambda)$ for the second-order dynamics described in (6). Note that, even though $\zeta = 0$ violates (16b), the requirement in (16a) does not depend on ζ. Notably, $g_i(\lambda)$ is Hurwitz if and only if (16a) is fulfilled. In fact, (16a) corresponds to the condition presented in Proposition 2, i.e., dropping the second requirement in (16) from Theorem 1 yields the convergence conditions for the second-order protocol (5).

4.4. Consensus in the presence of disturbances

The effect of disturbances is analyzed in this section. This analysis is conducted for the case of agents modeled as triple integrators, however, similarly to Lemma 2, it is straightforward to extend the results to any number of integrators.

Consider now that each agent is described by

$$\begin{cases} \dot{\theta}_i = \alpha_i \\ \dot{\alpha}_i = \beta_i \\ \dot{\beta}_i = \mu_i + d_i \end{cases}, \tag{18}$$

where $d_i \in \mathbb{R}$ is a disturbance acting on the ith agent, or equivalently, in vector form, that $\dddot{\boldsymbol{\theta}} = \boldsymbol{\mu} + \mathbf{d}$, where $\mathbf{d} = \left[d_1 \ \cdots \ d_n\right]^\top \in \mathbb{R}^n$ represents the disturbances acting on the system. Consider again the Lyapunov transformation introduced in (12), and recall that $\mathbf{V} = \left[\mathbf{v}_1 \ \cdots \ \mathbf{v}_n\right]$ and $\mathbf{V}^{-1} = \left[\mathbf{w}_1 \ \cdots \ \mathbf{w}_n\right]^\top$, with $\mathbf{v}_1 = \mathbf{1}_n$ and $\mathbf{w}_1 = \mathbf{r}$. Introduce $\mathbf{W} := \left[\mathbf{w}_2 \ \cdots \ \mathbf{w}_n\right]^\top$ and $\mathbf{Q} := \left[\mathbf{v}_2 \ \cdots \ \mathbf{v}_n\right]$, and note that the dynamics of $\boldsymbol{\theta}^*$ for the feedback actuated system can now be written as

$$\begin{cases} \dddot{\theta}_1^* = \mathbf{r}^\top \mathbf{d} & \text{(a)} \\ \dddot{\boldsymbol{\theta}}_{2,n}^* = -\mathbf{J}^* \left(\gamma \ddot{\boldsymbol{\theta}}_{2,n}^* + \dot{\boldsymbol{\theta}}_{2,n}^* + \zeta \boldsymbol{\theta}_{2,n}^*\right) + \mathbf{W}\mathbf{d} & \text{(b)} \end{cases}, \tag{19}$$

with $\boldsymbol{\theta}_{2,n}^* = \mathbf{W}\boldsymbol{\theta} = \left[\theta_2^* \ \dots \ \theta_n^*\right]^\top$. As previously mentioned, it follows from (13) that θ_1^* corresponds to the consensus value and $\boldsymbol{\theta}_{2,n}^*$ can be regarded as a transformed consensus error, meaning that consensus is reached if and only if $\boldsymbol{\theta}_{2,n}^* \to \mathbf{0}$. More concretely, it is possible to write $\boldsymbol{\theta}(t) = \mathbf{1}_n \theta_c(t) + \tilde{\boldsymbol{\theta}}(t)$ where $\theta_c(t) = \theta_1^*(t) = \mathbf{r}^\top \boldsymbol{\theta}(t)$ is the consensus value and $\tilde{\boldsymbol{\theta}}(t) = \mathbf{Q}\boldsymbol{\theta}_{2,n}^*(t)$ is the consensus error. Furthermore, consider the decomposition $\mathbf{d} = \bar{d}\mathbf{1}_n + \tilde{\mathbf{d}}$, where $\tilde{\mathbf{d}} := \left(\mathbf{I}_n - \mathbf{1}_n \mathbf{1}_n^\top / n\right)\mathbf{d}$, and note that $\mathbf{W}\mathbf{d} = \mathbf{W}\tilde{\mathbf{d}}$, because $\mathbf{W}\mathbf{1}_n = \mathbf{0}$. Therefore, the dynamics (19b) can be written as

$$\dot{\tilde{\mathbf{x}}} = \mathbf{H}(\mathbf{J}^*)\tilde{\mathbf{x}} + \tilde{\mathbf{B}}\tilde{\mathbf{d}}, \tag{20}$$

where $\tilde{\mathbf{B}} := \left[\mathbf{0} \ \ \mathbf{0} \ \ \mathbf{W}^\top\right]^\top$ and $\tilde{\mathbf{x}} = \left(\mathbf{I}_3 \otimes \mathbf{W}\right)\mathbf{x}$.

The following result describes a sufficient condition for consensus in the presence of disturbances.

Proposition 4. *The consensus protocol (8) for triple integrator agents achieves consensus in the presence of the disturbances* $\mathbf{d}$ *if the entries of* $\mathbf{d}$ *are all equal and the conditions presented in Theorem 1 are fulfilled.*

Proof. Consensus is reached if and only if $\boldsymbol{\theta}_{2,n}^* \to \mathbf{0}$, which holds if and only if the origin of (19b) is asymptotically/ exponentially stable. The latter is true if the conditions described in Theorem 1 hold and $\mathbf{W}\mathbf{d} = \mathbf{0}$, or equivalently, $\tilde{\mathbf{d}} = \mathbf{0}$, meaning that $\mathbf{d} = d\mathbf{1}_n$. □

The following result holds when the disturbances are not all equal, i.e., when $\tilde{\mathbf{d}} \neq \mathbf{0}$, and shows that robust consensus can be achieved, in the sense bounded disturbances lead to bounded consensus errors.

Proposition 5. *If* $\tilde{\mathbf{d}}(t)$ *is bounded, i.e.,* $\|\tilde{\mathbf{d}}(t)\| \leq D$ *for all* t, *and the conditions from Theorem 1 hold, then the disturbances* $\mathbf{d}$ *lead to a bounded consensus error and do not cause instability. Concretely, if* $\|\tilde{\mathbf{d}}(t)\|_p \leq D_p$ *for some* l_p*-norm, then a bound is given by* $\|\tilde{\boldsymbol{\theta}}(t)\|_p \leq z_p(t)$, *with*

$$z_p(t) := \|\tilde{\mathbf{C}} e^{\mathbf{H}(\mathbf{J}^*)t} \tilde{\mathbf{x}}(0)\|_p + \left(\int_0^\infty \|\tilde{\mathbf{C}} e^{\mathbf{H}(\mathbf{J}^*)s} \tilde{\mathbf{B}}\|_p \, ds\right) D_p,$$

where $\tilde{\mathbf{C}} = [\mathbf{Q} \ \ \mathbf{0} \ \ \mathbf{0}]$.

Proof. When the conditions from Theorem 1 hold, the system described by (20) is input-to-state stable with $\tilde{\mathbf{d}}$ as input. Therefore, if $\|\tilde{\mathbf{d}}(t)\|_p \leq D_p$ for all $t \geq 0$, then the state $\tilde{\mathbf{x}}$ is ultimately bounded and the ultimate bound is a function of D_p. Consequently, the consensus error $\tilde{\boldsymbol{\theta}} = \mathbf{Q}\boldsymbol{\theta}_{2,n}^* = \tilde{\mathbf{C}}\tilde{\mathbf{x}}$ is also ultimately bounded. The proposed bound follows directly from the solution of (20). □

When the disturbances are constant, a more detailed analysis can be conducted, yielding the following result.

Proposition 6. *The consensus protocol (8) for triple integrator agents achieves consensus in the presence of constant disturbances* $\mathbf{d}$ *if and only if all the entries of* $\mathbf{d}$ *are equal and the conditions presented in Theorem 1 are fulfilled. Moreover, when the entries of* $\mathbf{d}$ *are not all equal, consensus is still achieved for* $\boldsymbol{\alpha}$ *and* $\boldsymbol{\beta}$. *More concretely, for large* t,

$$\boldsymbol{\theta}(t) \to \mathbf{1}_n \mathbf{r}^\top \left(\boldsymbol{\theta}(0) + \boldsymbol{\alpha}(0)t + \boldsymbol{\beta}(0)\frac{t^2}{2!} + \mathbf{d}\frac{t^3}{3!}\right) + \tilde{\boldsymbol{\theta}}_\infty, \tag{21}$$

with

$$\tilde{\boldsymbol{\theta}}_\infty = \frac{1}{\zeta}\mathbf{Q}\left(\mathbf{J}^*\right)^{-1}\mathbf{W}\mathbf{d}$$

where $\mathbf{r}$ *is the non-negative left eigenvector of* $\mathbf{L}$ *associated to the null eigenvalue, such that* $\mathbf{1}_n^\top \mathbf{r} = 1$.

Proof. Considering constant disturbances, it is straightforward to solve (19a), yielding

$$\theta_1^*(t) = \theta_1^*(0) + \alpha_1^*(0)t + \beta_1^*(0)\frac{t^2}{2!} + \mathbf{r}^\top \mathbf{d}\frac{t^3}{3!}.$$

Note that if $\mathbf{d}$ is constant, (19b) can be rewritten as an error system with $\tilde{\boldsymbol{\theta}}_{2,n}^* = \boldsymbol{\theta}_{2,n}^* - (\zeta\mathbf{J}^*)^{-1}\mathbf{W}\mathbf{d}$ and its first and second time derivatives as state variables. It follows immediately that the origin of this new error system is exponentially stable, meaning that $\boldsymbol{\theta}_{2,n}^* \to (\zeta\mathbf{J}^*)^{-1}\mathbf{W}\mathbf{d}$. It is now possible to transform the solution back to the original system variables. Recalling that $\theta_1^* = \mathbf{r}^\top\boldsymbol{\theta}$, $\alpha_1^* = \mathbf{r}^\top\boldsymbol{\alpha}$, and $\beta_1^* = \mathbf{r}^\top\boldsymbol{\beta}$, one finally obtains that for large t, (21) holds. To conclude that consensus is achieved for state variables $\boldsymbol{\alpha}$ and $\boldsymbol{\beta}$, simply note that $\boldsymbol{\alpha} = \dot{\boldsymbol{\theta}}$, $\boldsymbol{\beta} = \ddot{\boldsymbol{\theta}}$ and $\tilde{\boldsymbol{\theta}}_\infty = \mathbf{0}$. □

4.5. Illustrative examples

Some examples are now presented considering three different interaction topologies, as described by the digraphs presented in Fig. 2. First, the convergence to consensus without the presence of disturbances is addressed, in order to illustrate the convergence criteria described in

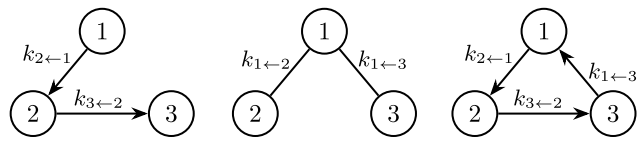

(a) Leader-follower. (b) Undirected. (c) Cycle.

Fig. 2. Digraphs associated with the interaction topologies that are addressed in the examples.

Theorem 1, and then an example considering disturbances is given, to validate the results presented in Section 4.4.

Unless otherwise stated, in the remainder of this section it is considered that $k_{i\leftarrow j} = 1$ and $\gamma = 1$, and that $\theta_i(0) = 10(i-1)$, $\alpha_i(0) = -0.5(i-1)$, and $\beta_i(0) = 0.05i$.

4.5.1. Leader-follower topology

When an agent has only outgoing interaction links, without any incoming ones, that agent is called leader and the others are called followers. Without loss of generality, one can label the leader as agent 1. An example of a leader-follower topology is given by the digraph illustrated in Fig. 2(a). The matrix $\mathbf{L}$ associated to that digraph is then

$$\mathbf{L} = \begin{bmatrix} 0 & 0 & 0 \\ -1 & 1 & 0 \\ 0 & -1 & 1 \end{bmatrix}.$$

If it is noted that matrix $\mathbf{L}$ can be transformed into a triangular matrix by a relabeling of the digraph vertices (Ren & Atkins, 2007), it can be concluded that all the eigenvalues of $\mathbf{L}$ are real. In this case, the stability bounds are given in Corollary 1. It is worth noting that the input of the leader agent is null, i.e., $\mu_1 = 0$ (its neighborhood is the empty set). Then, according to the agent dynamics (7), it is concluded that $\theta_1(t) = \theta_1(0) + \alpha_1(0)t + \beta_1(0)\frac{t^2}{2}$. Therefore, when consensus is achieved, all agents must converge to these values, i.e.,

$$\boldsymbol{\theta}(t) \to \mathbf{1}_n \left(\theta_1(0) + \alpha_1(0)t + \beta_1(0)\frac{t^2}{2}\right),$$

as it can be observed in Fig. 3(a). Then, by comparison with the consensus values presented in Lemma 2, it is possible to draw the conclusion that for a leader-follower topology where the leader is agent 1, $\mathbf{r} = \mathbf{e}_1$.

The evolution of the state of the agents with time, for the interaction topology described by the digraph of Fig. 2(a), is presented in Fig. 3 for $\zeta = 0.5$, $\zeta = 1$, and $\zeta = 1.5$. Recall that $\gamma = 1$ and note that non-null eigenvalues of $\mathbf{L}$ are $\eta_2 = \eta_3 = 1$. Then, in order to reach consensus, according to Corollary 1, ζ must be smaller than one. Clearly, when $\zeta = 0.5$ the bound on ζ is verified and the agents reach consensus, and when $\zeta = 1.5$ the bound on ζ is not verified and the system becomes unstable. For the critical condition of $\zeta = 1$, one would expect that the system became marginally stable. However, Fig. 3(b) suggests that the system is unstable. In fact, this exact condition leads to two pairs of coincident poles in the imaginary axis, which is in accordance with the evolution presented in Fig. 3(b), that shows linearly growing oscillations.

4.5.2. Undirected topology

The case of an undirected interaction topology, as the one described by the digraph of Fig. 2(b), is now addressed. In this case, $\mathbf{L}$ is a symmetric matrix and therefore all its eigenvalues are real. In this example,

$$\mathbf{L} = \begin{bmatrix} 2 & -1 & -1 \\ -1 & 1 & 0 \\ -1 & 0 & 1 \end{bmatrix}.$$

As in the previous example, it is possible to determine the vector $\mathbf{r}$, which is in this case $\mathbf{r} = \frac{1}{n}\mathbf{1}_n$. To draw that conclusion, recall the definition of $\mathbf{r}$ and note that is equivalent to saying that $\mathbf{r}$ is the right eigenvector of $\mathbf{L}^\top$ associated with the null eigenvalue, such that $\mathbf{1}_n^\top \mathbf{r} = 1$. The result follows by noting that, in this case, it holds that $\mathbf{L}^\top = \mathbf{L} \implies \mathbf{L}^\top \mathbf{1}_n = \mathbf{0}$. It follows from Lemma 2 that for $\mathbf{r} = \frac{1}{n}\mathbf{1}_n$ the consensus value will be determined by the average of the initial conditions.

The evolution of the agents for the undirected topology is presented in Fig. 4, again for $\zeta = 0.5$, $\zeta = 1$, and $\zeta = 1.5$. The non-null eigenvalues of $\mathbf{L}$ are now $\eta_2 = 1$ and $\eta_3 = 3$. Then, the conditions for reaching consensus are $\gamma > 0$ and $\zeta < \gamma$. Considering again $\gamma = 1$ one obtains $\zeta < 1$, as in the previous example. Fig. 4(a) presents the case when $\zeta = 0.5$ (in which the bound on ζ is verified) and it is clear that the group of agents reaches a consensus. The case when $\zeta = 1.5$ (the bound on ζ is not verified) is presented in Fig. 4(c) and, clearly, the system becomes unstable and the agents do not reach consensus. For the critical condition of $\zeta = 1$, the system becomes marginally stable, as evidenced by the undamped oscillations present in the evolution that can be seen in Fig. 4(b).

4.5.3. Cycle topology

Finally, the case of a cyclic interaction topology, as the one described by the digraph of Fig. 2(c), is addressed. This is perhaps the most interesting of the three cases. In this example, the Laplacian matrix is given by

$$\mathbf{L} = \begin{bmatrix} 1 & 0 & -1 \\ -1 & 1 & 0 \\ 0 & -1 & 1 \end{bmatrix}.$$

Notably, the eigenvalues of $\mathbf{L}$ contain an imaginary part. Fax and Murray (2004) show that for a cyclic topology, the eigenvalues of $\mathbf{L}$ are given by

$$\eta_i = 1 - \exp\left(j\frac{2\pi(i-1)}{n}\right)$$

for $i = 1, \dots, n$. This means that, besides the null eigenvalue, given by $i = 1$, the remainder eigenvalues will be $\eta_\pm = 3/2 \pm j\sqrt{3}/2$. It follows from Theorem 1 that in order for consensus to be achieved, it must be $\gamma > \sqrt{6}/6$. Considering that $\gamma = 1$, as in the previous cases, the condition $\zeta < \zeta_c$, with $\zeta_c := \left(6 - \sqrt{6}\right)/3$ is now obtained.

For a cyclic digraph as the one presented in Fig. 2(c), with equal connection weights (in this case, $k_{i\leftarrow j} = 1$), it holds that $\mathbf{r} = \frac{1}{n}\mathbf{1}_n$, as in the case of the undirected topology. To conclude this, note that

$$\sum_{i=1}^{n} \mu_i = 0 \implies \frac{1}{n}\sum_{i=1}^{n} \dot{\beta}_i = 0 \implies \bar{\beta}(t) = \bar{\beta}(0).$$

But from Lemma 2, $\boldsymbol{\beta}(t) \to \mathbf{1}_n \mathbf{r}^\top \boldsymbol{\beta}(0)$. Therefore, one concludes that $\mathbf{r} = \frac{1}{n}\mathbf{1}_n$.

In Fig. 5, the time evolution of the agents is presented for $\zeta = 0.5$, $\zeta = \zeta_c$, and $\zeta = 1.5$. When $\zeta = 0.5$, the bounds on ζ and γ are fulfilled and therefore the agents reach consensus, as can be observed in Fig. 5(a). For $\zeta = 1.5$, the bound on ζ is not verified and the agents diverge, as can be seen in Fig. 5(c). Regarding the critical condition, $\zeta = \zeta_c$, the system becomes marginally stable, leading to the undamped oscillations that can be observed in Fig. 5(b) and the agents do not reach consensus.

4.5.4. Cycle topology in the presence of disturbances

Some examples are now presented considering the interaction topology of the digraph in Fig. 2(c), with $\gamma = 1.2$ and $\zeta = 0.4$, to illustrate the effect of disturbances and validate the results introduced in Propositions 5 and 6.

The evolution of the states of the agents for these examples is presented in Fig. 6. Fig. 6(a) presents the evolution in the absence of disturbances. Figs. 6(b)–6(d) present the response for different constant

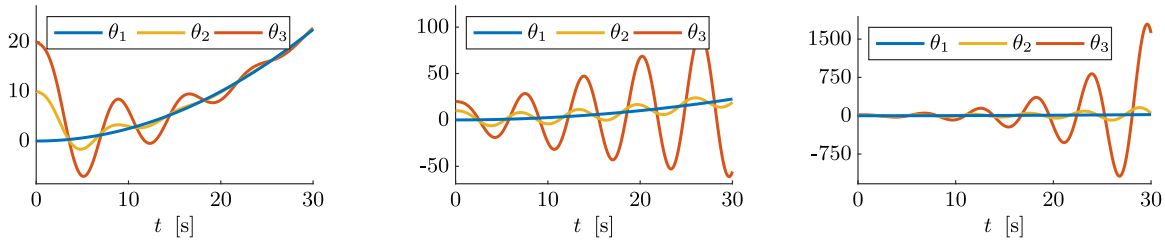

(a) Evolution for $\zeta = 0.5$. (b) Evolution for $\zeta = 1$. (c) Evolution for $\zeta = 1.5$.

Fig. 3. Evolution of the states of the agents for interaction topology presented in Fig. 2(a).

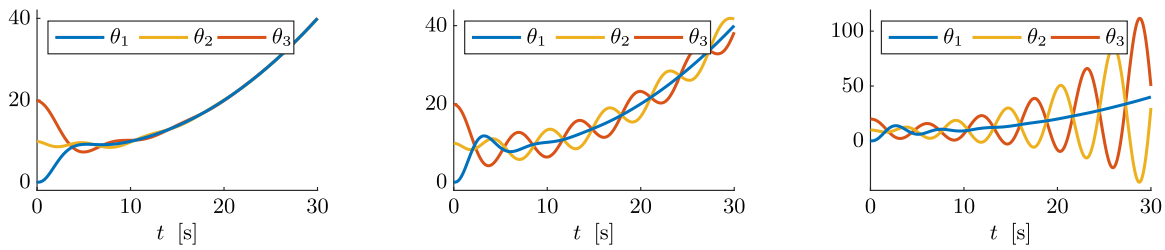

(a) Evolution for $\zeta = 0.5$. (b) Evolution for $\zeta = 1$. (c) Evolution for $\zeta = 1.5$.

Fig. 4. Evolution of the states of the agents for interaction topology presented in Fig. 2(b).

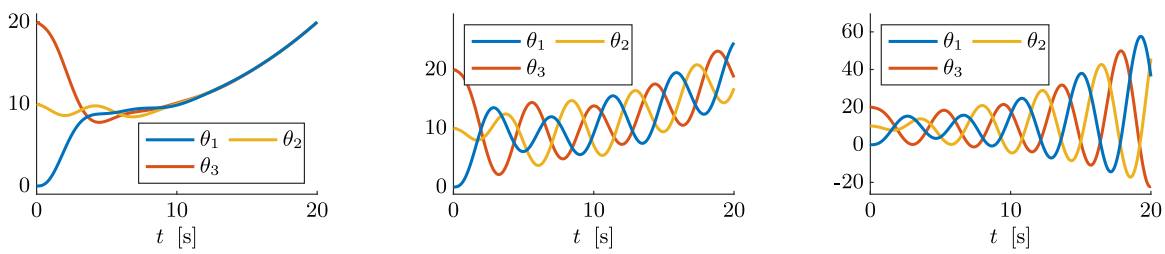

(a) Evolution for $\zeta = 0.5$. (b) Evolution for $\zeta = \zeta_c$. (c) Evolution for $\zeta = 1.5$.

Fig. 5. Evolution of the states of the agents for interaction topology presented in Fig. 2(c).

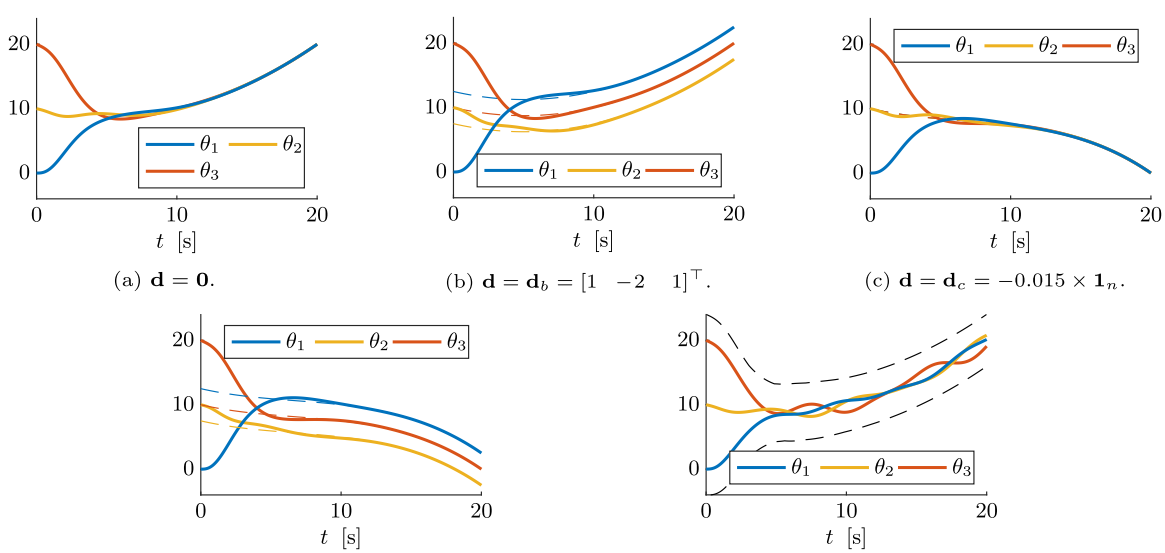

(a) $\mathbf{d} = \mathbf{0}$. (b) $\mathbf{d} = \mathbf{d}_b = [1 \quad -2 \quad 1]^\top$. (c) $\mathbf{d} = \mathbf{d}_c = -0.015 \times \mathbf{1}_n$.

(d) $\mathbf{d} = \mathbf{d}_b + \mathbf{d}_c = -0.015 \times \mathbf{1}_n + [1 \quad -2 \quad 1]^\top$. (e) $\mathbf{d}(t) = [1 \quad 0 \quad -1]^\top \left(\cos\left(\frac{7}{5}t + 2\right) + \cos\left(\frac{3}{4}t\right)\right)$.

Fig. 6. Evolution of the states of the agents in the presence of different disturbances, considering the topology from Fig. 2(c).

disturbances, and the dashed lines in these figures represent where the agents converge to, i.e., according to Proposition 6,

$$\boldsymbol{\theta}(t) \to \mathbf{1}_n \mathbf{r}^\top \left(\boldsymbol{\theta}(0) + \boldsymbol{\alpha}(0)t + \boldsymbol{\beta}(0)\frac{t^2}{2!} + \mathbf{d}\frac{t^3}{3!} \right) + \tilde{\boldsymbol{\theta}}_\infty.$$

Recall that in this case $\mathbf{r} = \frac{1}{n}\mathbf{1}_n$, to conclude that $\mathbf{r}^\top\mathbf{d}$ is equal to the average of the entries of $\mathbf{d}$.

In Fig. 6(b), the disturbance $\mathbf{d}$ was chosen such that $\mathbf{r}^\top\mathbf{d} = 0$ and $\tilde{\boldsymbol{\theta}}_\infty \neq \mathbf{0}$. With $\mathbf{d} = \mathbf{d}_b = [1 \quad -2 \quad 1]^\top$, it follows that $\tilde{\boldsymbol{\theta}}_\infty = \tilde{\boldsymbol{\theta}}_b = [2 \quad -2 \quad 0]^\top$. Since $\mathbf{r}^\top\mathbf{d} = 0$, then

$$\boldsymbol{\theta}(t) \to \mathbf{1}_n \left(\bar{\theta}(0) + \bar{\alpha}(0)t + \bar{\beta}(0)\frac{t^2}{2!} \right) + \tilde{\boldsymbol{\theta}}_b.$$

In Fig. 6(c), $\mathbf{d}$ was chosen such that $\tilde{\boldsymbol{\theta}}_\infty = \mathbf{0}$ and $\mathbf{r}^\top\mathbf{d} \neq 0$, i.e., all the entries of $\mathbf{d}$ are equal and non-null ($\mathbf{d} = \mathbf{d}_c = d\mathbf{1}_n$ with $d = -0.015$). In this case,

$$\boldsymbol{\theta}(t) \to \mathbf{1}_n \left(\bar{\theta}(0) + \bar{\alpha}(0)t + \bar{\beta}(0)\frac{t^2}{2!} + d\frac{t^3}{3!} \right),$$

and the agents reach consensus. In Fig. 6(d), $\mathbf{d} = \mathbf{d}_b + \mathbf{d}_c$ is considered, hence both effects are present. Therefore,

$$\boldsymbol{\theta}(t) \to \mathbf{1}_n \left(\bar{\theta}(0) + \bar{\alpha}(0)t + \bar{\beta}(0)\frac{t^2}{2!} + d\frac{t^3}{3!} \right) + \tilde{\boldsymbol{\theta}}_b.$$

Finally, a bounded disturbance is considered in Fig. 6(e), to illustrate the result introduced in Proposition 5. Particularly, the disturbance $\mathbf{d}$ was chosen to be $\mathbf{d} = \mathbf{d}_e(t) = \mathbf{u}f(t)$, where $\mathbf{u} = [1 \quad 0 \quad -1]^\top$ and $f(t) = \cos\left(\frac{7}{5}t + 2\right) + \cos\left(\frac{3}{4}t\right)$. The dashed lines in Fig. 6(e) represent a bound on the states of the agents, built using the bound provided in Proposition 5. Concretely, recall that $\boldsymbol{\theta}(t) = \mathbf{1}_n\theta_c(t) + \tilde{\boldsymbol{\theta}}(t)$ (or component-wise, $\theta_i(t) = \theta_c(t) + \tilde{\theta}_i(t)$) to write that

$$|\theta_i(t) - \theta_c(t)| = |\tilde{\theta}_i(t)| \leq \|\tilde{\boldsymbol{\theta}}(t)\|_\infty \leq z_\infty(t),$$

where the bound provided in Proposition 5 is used with $p = \infty$. This leads to

$$\theta_c(t) - z_\infty(t) \leq \theta_i(t) \leq \theta_c(t) + z_\infty(t),$$

which are the bounds presented in Fig. 6(e). Moreover, note that for $\mathbf{d} = \mathbf{d}_e(t)$ it holds that $\tilde{\mathbf{d}} = \mathbf{d}$. Therefore, since $|f(t)| \leq F$ for all t, for some $F \in \mathbb{R}^+$, then $\|\tilde{\mathbf{d}}(t)\|_\infty \leq F$ for all t.

5. Formation control

This section tackles the problem of designing a formation tracking controller for double-integrator modeled vehicles, enhanced with the ability to reject constant disturbances. To that end, the third-order consensus protocol (8) is used to augment a formation control law used for double-integrator vehicles with integral action, yielding a PID-like controller.

5.1. Formation tracking controller

Consider the system of n vehicles with the dynamics described in (1), ignoring for the moment the effect of the disturbance $\mathbf{d}_i$. Let $\tilde{\mathbf{p}}_i := \mathbf{p}_i - \mathbf{p}_i^{\mathbf{d}}$ be the trajectory tracking error. Then

$$\begin{cases} \dot{\mathbf{p}}_i = \mathbf{v}_i \\ \dot{\mathbf{v}}_i = \mathbf{u}_i \end{cases} \implies \begin{cases} \dot{\tilde{\mathbf{p}}}_i = \dot{\mathbf{p}}_i - \dot{\mathbf{p}}_i^{\mathbf{d}} := \tilde{\mathbf{v}}_i \\ \dot{\tilde{\mathbf{v}}}_i = \dot{\mathbf{v}}_i - \ddot{\mathbf{p}}_i^{\mathbf{d}} := \tilde{\mathbf{u}}_i \end{cases}. \tag{22}$$

Recall that, in order to track a prescribed formation, the goal is to have $\mathbf{p}_{ij} - \mathbf{p}_{ij}^{\mathbf{d}} \to \mathbf{0}$, where $\mathbf{p}_{ij}$ and $\mathbf{p}_{ij}^{\mathbf{d}}$ denote the relative position, and the desired relative position of vehicle i with respect to vehicle j, respectively. However, note that $\mathbf{p}_{ij} - \mathbf{p}_{ij}^{\mathbf{d}} = \tilde{\mathbf{p}}_i - \tilde{\mathbf{p}}_j$, meaning that, the goal is equivalent to $\tilde{\mathbf{p}}_i - \tilde{\mathbf{p}}_j \to \mathbf{0}$. The dynamics described in (22) are decoupled, and so, the controllers can be designed independently for each axis. Comparing the dynamics over each axis with the ones described in (4), it is possible to conclude they are the same. Also, note that the control objective is the same as the one described for protocol (5). Therefore, the consensus protocol (5) can be used to achieve formation tracking, and the control input $\tilde{\mathbf{u}}_i$ for the error dynamics becomes

$$\tilde{\mathbf{u}}_i = -\sum_{j\in\mathcal{N}_i} k_{i\leftarrow j}\left[\left(\tilde{\mathbf{p}}_i - \tilde{\mathbf{p}}_j\right) + \gamma\left(\tilde{\mathbf{v}}_i - \tilde{\mathbf{v}}_j\right)\right],$$

which is guaranteed to drive the vehicles into formation, under the conditions of Proposition 2. The control input for the ith vehicle can then be recovered, yielding

$$\mathbf{u}_i = \ddot{\mathbf{p}}_i^{\mathbf{d}} - \sum_{j\in\mathcal{N}_i} k_{i\leftarrow j}\left[\left(\mathbf{p}_{ij} - \mathbf{p}_{ij}^{\mathbf{d}}\right) + \gamma\left(\mathbf{v}_{ij} - \dot{\mathbf{p}}_{ij}^{\mathbf{d}}\right)\right]. \tag{23}$$

The same rationale could be used to define a controller for vehicles modeled as triple integrators using the consensus protocol (8).

5.1.1. Inclusion of integral action

When performing formation tracking, using the control law described in (23), the distributed multi-vehicle system is able to track the prescribed formation, under the conditions of Proposition 2. However, real systems are susceptible to a number of non-idealities, such as disturbances, modeling errors and actuator dead-zones, which can deteriorate the ability to achieve their goal.

Recover now the disturbances $\mathbf{d}_i$ in the system of n vehicles with the dynamics described in (1), which were previously ignored. To mitigate the effects of these disturbances, integral action is proposed. This can be achieved considering the integral of the position tracking error, modeled by an extra state $\tilde{\mathbf{g}}_i$, described by $\dot{\tilde{\mathbf{g}}}_i = \tilde{\mathbf{p}}_i$. The error system described in (22), considering this new state and the disturbances that were previously ignored becomes

$$\begin{cases} \dot{\tilde{\mathbf{g}}}_i = \tilde{\mathbf{p}}_i \\ \dot{\tilde{\mathbf{p}}}_i = \tilde{\mathbf{v}}_i \\ \dot{\tilde{\mathbf{v}}}_i = \tilde{\mathbf{u}}_i + \mathbf{d}_i \end{cases}.$$

This is now a triple integrator system with a constant disturbance, analogous to the one in (18). It is then straightforward to conclude that the consensus protocol (8) can be used to derive the control law

$$\tilde{\mathbf{u}}_i = -\sum_{j\in\mathcal{N}_i} k_{i\leftarrow j}\left[\left(\tilde{\mathbf{p}}_i - \tilde{\mathbf{p}}_j\right) + \gamma\left(\tilde{\mathbf{v}}_i - \tilde{\mathbf{v}}_j\right) + \zeta\left(\tilde{\mathbf{g}}_i - \tilde{\mathbf{g}}_j\right)\right]$$

for the error dynamics, that is able to track the formation in the presence of constant disturbances, as stated in Proposition 6, when the conditions of Theorem 1 hold. Finally, noting that

$$\tilde{\mathbf{g}}_i - \tilde{\mathbf{g}}_j = \int_{t_0}^{t}\left(\tilde{\mathbf{p}}_i - \tilde{\mathbf{p}}_j\right)dt = \int_{t_0}^{t}\left(\mathbf{p}_{ij} - \mathbf{p}_{ij}^{\mathbf{d}}\right)dt,$$

the control input for the ith vehicle is recovered, yielding

$$\begin{aligned} \mathbf{u}_i = \ddot{\mathbf{p}}_i^{\mathbf{d}} - \sum_{j\in\mathcal{N}_i} k_{i\leftarrow j}\Bigg[& \left(\mathbf{p}_{ij} - \mathbf{p}_{ij}^{\mathbf{d}}\right) \\ & + \gamma\left(\mathbf{v}_{ij} - \dot{\mathbf{p}}_{ij}^{\mathbf{d}}\right) + \zeta\int_{t_0}^{t}\left(\mathbf{p}_{ij} - \mathbf{p}_{ij}^{\mathbf{d}}\right)dt\Bigg]. \end{aligned} \tag{24}$$

5.1.2. Inclusion of goal seeking terms

Having designed a controller that achieves formation tracking, it is important to modify this controller in a way that all vehicles are driven to their desired positions, i.e., that $\mathbf{p}_i \to \mathbf{p}_i^{\mathbf{d}}$. Note that the formation is prescribed by the position of each vehicle with respect to the others, meaning that vehicles can achieve formation tracking without reaching their desired positions. As an example, in a limit case, aerial vehicles could be in formation while at free-fall, because the relative positions remain the same.

To drive the vehicles to their desired positions, the previously derived control law must be modified by adding what are called goal seeking terms. These terms consist of trajectory tracking controllers that "attract" the vehicles to their desired positions. Note that, to implement

such controllers, the vehicles must have knowledge of their own state, and not only their state with respect to their neighbors. In a way, the goal seeking term represents the knowledge a vehicle has of its own state. In terms of the digraph, this knowledge can be represented by a self-loop, that models the information flow from a vehicle to itself, i.e., the vehicle sees/senses itself. In contrast with the work by Ren and Atkins (2007), this work considers adding goal seeking terms only to a limited set of vehicles $\mathcal{V}_S$. These vehicles track their desired trajectory, and the others adjust their trajectories by tracking the formation. As such, not all vehicles need to have knowledge of their own state.

In short, one seeks to add a PID trajectory tracking controller, of the form

$$\tilde{\mathbf{u}}_i^G = -k_{i\leftarrow i}\left(\tilde{\mathbf{p}}_i + \gamma\tilde{\mathbf{v}}_i + \zeta\int\tilde{\mathbf{p}}_i\,dt\right),$$

to the previously derived control law, seeking to ensure that $\tilde{\mathbf{p}}_i \to \mathbf{0}$ as $t \to \infty$. Analogously, one can analyze adding the term

$$\mu_i^G = -k_{i\leftarrow i}\left[\alpha_i + \gamma\beta_i + \zeta\theta_i\right],$$

to μ_i in the consensus protocol (8) to drive the system (7) to the origin. Note that now, the control for system (7) can be written in vector form as $\boldsymbol{\mu} = -\boldsymbol{\mathcal{L}}\boldsymbol{\alpha} - \gamma\boldsymbol{\mathcal{L}}\boldsymbol{\beta} - \zeta\boldsymbol{\mathcal{L}}\boldsymbol{\theta}$, and the feedback actuated system becomes $\dot{\mathbf{x}} = \mathbf{H}(\boldsymbol{\mathcal{L}})\mathbf{x}$, where $\boldsymbol{\mathcal{L}}$ is the generalized Laplacian of the digraph. The goal seeking terms seek to ensure that the feedback actuated system, now described by $\dot{\mathbf{x}} = \mathbf{H}(\boldsymbol{\mathcal{L}})\mathbf{x}$, is stable, i.e., that $\mathbf{H}(\boldsymbol{\mathcal{L}})$ is a stable matrix.

Theorem 2. *Suppose that the communication digraph has a spanning tree. Then, the vehicles reach their desired positions if and only if there is at least a vehicle with a goal seeking term that has a directed path to all others, and the coupling gains γ and ζ satisfy the conditions for consensus (16a) and (16b) of Theorem 1, substituting the Laplacian $\mathbf{L}$ by the generalized Laplacian $\boldsymbol{\mathcal{L}}$.*

Proof. The vehicles reach their desired positions when the matrix $\mathbf{H}(\boldsymbol{\mathcal{L}})$ is Hurwitz. Recall Proposition 3 to relate the eigenvalues of $\mathbf{H}(\boldsymbol{\mathcal{L}})$ with the eigenvalues of $\boldsymbol{\mathcal{L}}$. Let $\eta_i \in \mathbb{C}$, $i = 1,\dots,n$ be the eigenvalues of $\boldsymbol{\mathcal{L}}$ and λ_{ij}, $j = 1,2,3$ be the eigenvalues of $\mathbf{H}(\boldsymbol{\mathcal{L}})$ associated with η_i, i.e., the roots $h_i(\lambda) = 0$, with $h_i(\lambda) = \lambda^3 + \eta_i\left(\gamma\lambda^2 + \lambda + \zeta\right)$. Since for each null eigenvalue in $\boldsymbol{\mathcal{L}}$, there are three null eigenvalues in $\mathbf{H}(\boldsymbol{\mathcal{L}})$, then for $\mathbf{H}(\boldsymbol{\mathcal{L}})$ to be Hurwitz there can be no null eigenvalue in $\boldsymbol{\mathcal{L}}$. Considering that, by hypothesis, the communication digraph contains a spanning tree, then by Proposition 1 there are no null eigenvalues in $\boldsymbol{\mathcal{L}}$ if and only if a vehicle that has a directed path to all others has a goal seeking term. Moreover, in that case, all eigenvalues of $\boldsymbol{\mathcal{L}}$ have positive real part. Therefore, the result presented in Lemma 4 can be applied to the third degree polynomial $h_i(\lambda)$ associated to an eigenvalue η_i of $\boldsymbol{\mathcal{L}}$. Finally, noting that all the roots of $h_i(\lambda)$ associated with the eigenvalues η_i of $\boldsymbol{\mathcal{L}}$ must have negative real part, the conditions that must be met are (16) and the proof is concluded. □

Remark 4. The results presented in Theorems 1 and 2 depend on the eigenvalues of the Laplacian $\mathbf{L}$ and generalized Laplacian $\boldsymbol{\mathcal{L}}$, respectively, which may raise scalability issues. The complexity on the computation of these eigenvalues is $O(n^3)$. Therefore, for large n, the computation of these eigenvalues might be computationally expensive. Nonetheless, this result targets the design of the protocol parameters γ and ζ, which can be done offline.

5.2. Illustrative example

Before applying the results presented in this section in an experimental setting, an illustrative example is presented. The interaction topology considered in this example is presented in Fig. 7, where the digraph is represented as a tree of strongly connected components, that will be referred to as supernodes. The depth M of the graph, as illustrated in Fig. 7(a), can be changed to scale the number of vehicles,

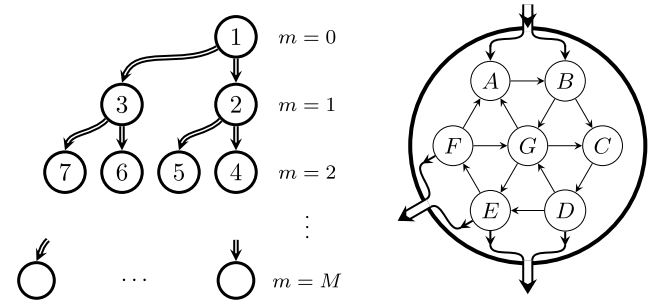

(a) Tree graph composed of supernodes. (b) Supernode.

Fig. 7. Description of the graph that models the interaction topology. Each node on the graph of Fig. 7(a) is a supernode, as the one presented in Fig. 7(b).

which is given by $n = 7\left(2^{M+1} - 1\right)$. For this example, $M = 3$ is considered, which leads to $n = 105$. Note that this graph contains a spanning tree, which is a necessary condition for consensus.

The only nodes that have a directed path to all others are the nodes in supernode 1 of Fig. 7(a) (the root supernode). It follows from Theorem 2 that at least one of those vehicle must have a goal-seeking term so that all vehicles reach their desired positions. Therefore, consider adding self-loops to nodes A and B of supernode 1. Finally, all the arc weights are set to $k_{i\leftarrow j} = 1.5$ and the coupling gains used are $\gamma = 2.5$ and $\zeta = 0.11$, which were chosen to verify the conditions from Theorem 2.

In this example, the vehicles are 2D double integrators equipped with the control law (24). Their goal is to move in the plane along the x-axis at a constant speed $v_x = 1\text{m/s}$, with a circle shaped formation. The initial positions of the vehicles are assigned to be the initial desired positions plus some error, drawn from a Gaussian distribution with expectation $\boldsymbol{\mu} = [0\ \ 1]^\top$ and covariance $\boldsymbol{\Sigma} = \mathbf{I}_2$. The vehicles G and C, from the supernodes 2 and 4, are subject to constant disturbances $\mathbf{d}_i = [0\ \ -3]^\top$.

The results of this example are presented in Fig. 8. The movement of the vehicles in the plane is presented in Fig. 8(a). There, it can be observed the convergence of the vehicles to the circle shaped formation, that moves at a constant speed of 1m/s along the x-axis. Fig. 8(b) presents a positive definite function of the position error given by

$$V(t) := \sum_{i=1}^{n}\left[k_{i\leftarrow i}^2\|\mathbf{p}_i - \mathbf{p}_i^{\mathbf{d}}\|^2 + \sum_{j\in\mathcal{N}_i} k_{i\leftarrow j}^2\|\mathbf{p}_{ij} - \mathbf{p}_{ij}^{\mathbf{d}}\|^2\right],$$

which goes to zero, meaning that the vehicles are able to track their desired positions in the presence of the constant disturbances.

6. Experimental validation

In this section, experimental results are presented to validate the proposed solutions. To that end, the presented algorithms were applied to multirotor vehicles. Nevertheless, these can be applied to any vehicles modeled as double integrators. In a first part, the application of these algorithms to multirotors is detailed. Then, the considered experimental setup is described, and finally the experimental results are presented.

6.1. Multirotor tracking control

Multirotor vehicles are characterized by having multiple rotors, all generating thrust aligned with the vertical direction of the vehicle. The multirotor dynamics can be modeled with different levels of complexity. An inner-outer loop control scheme is typically used to control the attitude (inner-loop) with actuation on the body torques, and the position of the multirotor (outer-loop) with actuation on the total thrust and virtual control inputs defined by the attitude. Under appropriate

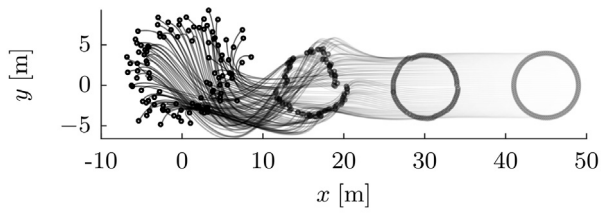

(a) Movement of the vehicles, with snapshots at $t = \{0, 15, 30, 45\}$s.

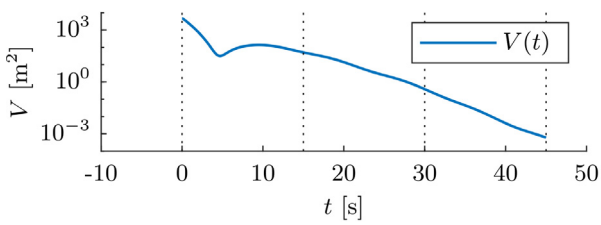

(b) Positive definite function of the position error.

Fig. 8. Results of the example, displayed up to time $t = 45$s.

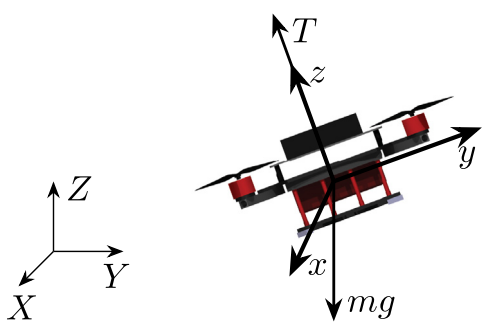

Fig. 9. Forces applied to the multirotor.

assumptions, it is adequate to use a 3-D double integrator to model the multirotor translational motion. More specifically, this model can be adopted if the attitude is controlled by an inner-loop attitude controller that is sufficiently fast, when compared to the outer-loop linear motion dynamics. This is a common approach which is used, for example, by Falanga et al. (2019).

To define the outer-loop position controller and ultimately apply the controller defined in Section 5, consider Newton's second law of motion, which states that $\sum_i \mathbf{f}_i = \dot{\mathbf{q}}$, where $\mathbf{f}_i \in \mathbb{R}^3$ represents the ith force applied to the multirotor, $m \in \mathbb{R}^+$ its mass, $\mathbf{v} \in \mathbb{R}^3$ its velocity, and $\mathbf{q} = m\mathbf{v}$ the linear momentum of the vehicle. Since the mass is constant, and considering the forces presented in Fig. 9,

$$\dot{\mathbf{v}} = \frac{1}{m}\sum_i \mathbf{f}_i = \frac{T}{m}\mathbf{R}\mathbf{e}_3 - g\mathbf{e}_3,$$

where g is the acceleration of gravity, $\mathbf{R}$ represents the rotation matrix from the body to the inertial frame and T represents the norm of the total thrust applied by the rotors. Note that, $\dot{\mathbf{v}} = \mathbf{u}$ is the control input of the double integrator system previously discussed. The goal is then to determine T, and the attitude associated with $\mathbf{R}$, that correspond to the control input $\mathbf{u}$.

Note that the matrix $\mathbf{R}$ can be decomposed into three rotation matrices, associated to a sequence of elementary rotations around the principal rotation axis. These rotations refer to the Euler angle representation of the orientation. Different rotation sequences can be used to represent an arbitrary rotation matrix $\mathbf{R}$. In this work, the ZYX Euler angle representation is adopted, for which $\mathbf{R}$ takes the form $\mathbf{R} = \mathbf{R}_z(\psi)\mathbf{R}_y(\theta)\mathbf{R}_x(\phi)$. For a rotation matrix, it holds that $\mathbf{R}^{-1} = \mathbf{R}^\top$. It follows that if (T, ϕ, θ) are chosen such that $\mathbf{R}_y(\theta)\mathbf{R}_x(\phi)T\mathbf{e}_3 = \mathbf{u}^*$, where $\mathbf{u}^* := m\mathbf{R}_z(\psi)^\top(\mathbf{u} + g\mathbf{e}_3)$, the double integrator model can be recovered. The angles ϕ and θ, as well as T, associated to $\mathbf{u}$, must then be determined. To do so, it is necessary to know ψ, commonly denoted by yaw angle. Note that the yaw angle varies with time, and can be controlled by providing the inner-loop attitude controller with a desired yaw angle, which was chosen to be constant. To determine ϕ, θ and T, given $\mathbf{u}$, ψ, and the transformed control input $\mathbf{u}^* = [u_1^* \; u_2^* \; u_3^*]^\top$, it can be written that

$$\frac{u_1^*}{u_3^*} = \tan(\theta), \quad \text{and} \quad \frac{u_2^*}{\sqrt{u_1^{*2} + u_3^{*2}}} = -\tan(\phi).$$

It is then straightforward to determine ϕ and θ, provided that either $u_1^* \neq 0$ or $u_3^* \neq 0$. To determine the total thrust, T, note that $T = \|\mathbf{u}^*\|$.

6.2. Experimental setup

In order to validate the proposed approach, experiments were conducted with multirotor vehicles in an indoor environment, using a motion capture system to acquire position data, which was then sent to the multirotors using WiFi. The Intel Aero Ready To Fly quadrotor was used, equipped with the PX4 autopilot. The capabilities of the autopilot were used for sensor fusion between the onboard sensors and the motion capture position and attitude data, and for interaction with the multirotor platform. The controllers were implemented in a single computer, which receives data from the multirotors and sends commands through WiFi. Due to space constraints, the experiments were conducted using two multirotors, while other multirotors were simulated in-the-loop, using the Gazebo simulator. The Robot Operating System (ROS) (more concretely, the MavROS package) was used as middleware for communication with the autopilot.

The flight procedure considers the takeoff for all vehicles simultaneously, using the capabilities of the PX4 autopilot, and only after all the multirotors are flying, a transition is made into the controller to test. When the experiment ends, all vehicles are given a command to land. The commands to switch between flight phases are manually inserted by the operator during the flight, and sent to all vehicles simultaneously.

6.3. Results

Experiments were performed to test the proposed control algorithms, and a video of these experiments is presented in https://youtu.be/99CGAzf4xDM. The goal is to compare the performance of the proposed control solution, that contemplates integral action with the baseline controller, without integral action. When presenting results, circles and squares are used to represent the current and initial positions of the vehicles, respectively. In the figures showing the altitude evolution, the shaded areas represent the takeoff and landing parts of the flight. In the middle area, the formation controller is active.

For these experiments, a leader vehicle is considered. This is a vehicle that only has outgoing links in the digraph that describes the interaction topology, and if there is a spanning tree in the digraph, this is also the only vehicle that has a directed path to all others. The trajectory tracking controller for the leader vehicle can be designed independently of the formation tracking controller. If the trajectory tracking controller for the leader is stable, and the formation tracking controller leads the vehicles into formation, then all vehicles are able to achieve their desired position. Without loss of generality, let the leader be vehicle 1. Since the controller for this vehicle can be designed independently, let this be given by

$$\mathbf{u}_1 = \ddot{\mathbf{p}}_1^{\mathbf{d}} - K_P\tilde{\mathbf{p}}_1 - K_V\tilde{\mathbf{v}}_1 - K_I\int_{t_0}^{t}\tilde{\mathbf{p}}_1\,dt, \tag{25}$$

which is a PID controller where $K_P, K_I, K_V \in \mathbb{R}^+$ are the proportional, integral, and derivative gains, respectively. Note that the control law

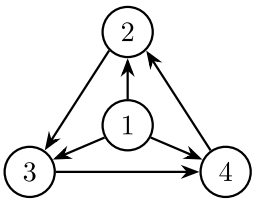

$$\mathbf{L} = 1.7 \begin{bmatrix} 0 & 0 & 0 & 0 \\ -1 & 2 & 0 & -1 \\ -1 & -1 & 2 & 0 \\ -1 & 0 & -1 & 2 \end{bmatrix}$$

Fig. 10. Interaction topology considered.

for the leader vehicle, which can be independently designed taking only into account its own state vector, consists in feedbacking all the error states associated to this vehicle. To tune the gains for this PID trajectory tracking controller, an LQR control design can be adopted.

In the prescribed motion, the leader follows a simple trajectory (going back and forth along a straight line with a sinusoidal velocity profile), and three other vehicles orbit the leader, at an altitude of one meter. This movement is slow and was carefully designed to fit the working space, with reasonable margins between the vehicles and the arena limits. The periodic motion considered has a period of 20 seconds, and was defined during two periods, i.e., 40 seconds. After those 40 seconds, the vehicles stop at the last desired position of this movement (which is also the initial position). This consists in a discontinuity on the desired motion, meaning that a new convergence is initiated at that instant. The digraph associated to the interaction topology considered is presented in Fig. 10. The connection weights are $k_{i\leftarrow j} = 1.7$, the derivative gain is $\gamma = 1.1\,\mathrm{s}^{-1}$, and the integral gain, when used, is $\zeta = 0.15\,\mathrm{s}^{-3}$, which can be verified to follow the conditions presented in Theorem 1. Due to the space constraints of the testing environment, the initial positions of the vehicles are close to their initial desired positions. However, they start with null velocity, so there is still a convergence to the desired time varying formation. The vehicles 2 and 4 are multirotors simulated in-the-loop using the Gazebo simulator, and the vehicles 1 and 3 are actual multirotors.

The movement on the horizontal plane, when integral action is not considered, is presented in Fig. 11(a) and in Fig. 11(b). After the initial convergence, the vehicles achieve the time varying formation in the horizontal plane, orbiting around the leader vehicle. The movement of the vehicles on the horizontal plane when considering integral action, is presented in Figs. 12(a) and 12(b). As can be observed, there are no noticeable differences between the movement on the horizontal plane with and without integral action, apart from the initial instants, which is also a consequence of slightly different initial positions.

Regarding the evolution of altitude with time, there is a clear distinction between the experiments with no integral action (Fig. 11(c)) and with integral action (Fig. 12(c)). Note that the presence of disturbances is confirmed when no integral action is present, as the vehicles climb to an altitude different than the desired altitude of one meter, and do not maintain the same altitude. This effect is apparent mainly in vehicle 3, which is one of the vehicles in the arena, and has influence on the other vehicles. The other vehicle in the arena (vehicle 1) plays the role of leader, using the trajectory tracking controller (25), and for that reason it is not influenced by the disturbance of vehicle 3. However, it can be noted that the leader vehicle is also subject to a disturbance, although its effect is smaller. Nonetheless, some influence is still noticeable, since when the experiment was performed without integral action on the formation tracking controller, the integral action of the trajectory tracking controller (25) was also not present (the integral gain K_I was set to zero). However, when performing the experiment with integral action on the formation tracking controller, K_I was set to $0.3\,\mathrm{s}^{-3}$, to reject the disturbance acting on the leader vehicle as well, enabling all vehicles to reach the desired altitude of one meter.

6.4. Discussion

The goal of this experiment was to assess the ability of the proposed integral action to reject disturbances, and verify that it provides increased capabilities when working with multirotor vehicles. These vehicles are susceptible to modeling errors, which can be interpreted as disturbances to the nominal system that is being considered. For this reason, when applying controllers to this type of vehicles, it is important to keep in mind that these must be designed with some robustness to these errors. It was shown that the ability of these vehicles to reach the prescribed formation is considerably influenced by these disturbances. These effects would be even more evident when considering an increased number of vehicles. In the described experiment, only two physical multirotors were used, and still, considerable improvements were observed when adding integral action. It is clear that the proposed integral action has a positive effect when performing formation control with multirotor vehicles. The effect of disturbances in multirotor vehicles is clearly more apparent on the vertical axis, as evidenced by the presented experiment. Since the system of double integrator agents previously described is decoupled, a choice could be made to add integral action to the vertical axis alone, as this is where most of the effect is visible. However, if flights were to be made in an open space, an interesting movement for the vehicles would be to move in formation with a constant velocity. In this case, if the velocity was high enough for the drag to have a considerable effect, it would probably be useful to add integral action to the controller on the other axis as well.

7. Concluding remarks

This paper proposed solutions to enhance the existing formation control algorithms for vehicles modeled as double integrators with the feature of integral action to enable disturbance rejection, which proved to be useful when working with multirotors. New theoretical results were achieved regarding the consensus-based protocols used

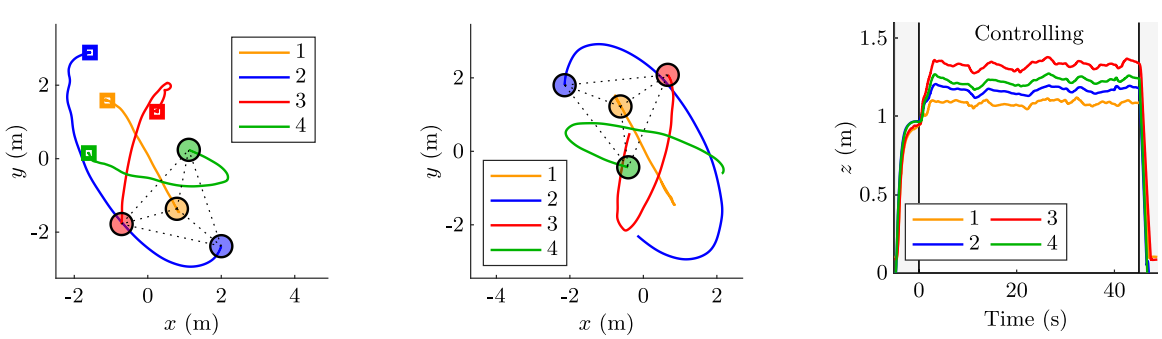

(a) Movement at $t = 11\,\mathrm{s}$. (b) Movement at $t = 22\,\mathrm{s}$. (c) Evolution of altitude with time.

Fig. 11. Results without integral action.

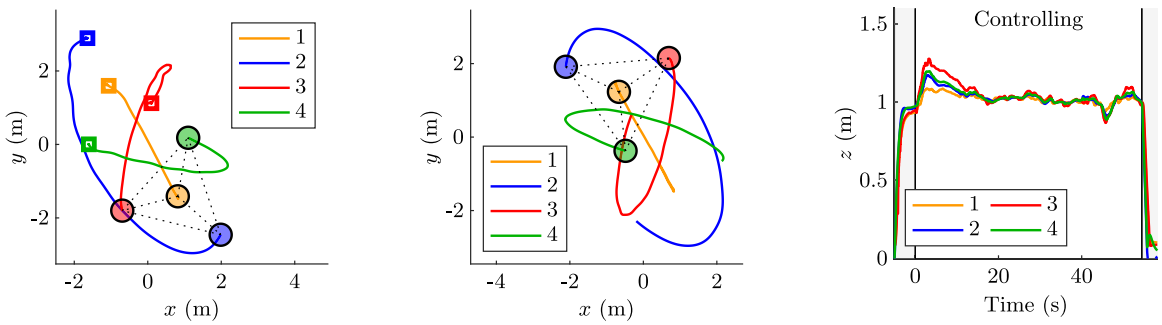

(a) Movement at $t = 11$ s. (b) Movement at $t = 22$ s. (c) Evolution of altitude with time.

Fig. 12. Results with integral action.

in this work. More concretely, novel criteria for the convergence of the third-order consensus protocol described by exact bounds on the coupling gains were obtained, describing necessary and sufficient conditions for convergence. The effect of disturbances acting on the agents was also analyzed for the third-order consensus protocol, although these results can easily be generalized for any order. These consensus protocols were used to design a formation tracking controller with constant disturbance rejection and the use of goal seeking terms was also analyzed. The algorithms were then tested on multirotors and experimental results were obtained, allowing to successfully validate the proposed approach. Specifically, it was shown that the proposed algorithm is able to reject constant disturbances acting on the vehicles, while following a decentralized approach, and considering a limited amount of information.

In the future, the authors intend to deepen the analysis of the proposed third-order consensus protocol considering, for example, the effect of actuator or network delays. Moreover, the authors also wish to consider the design of the protocol parameters under the framework of optimal control theory.

Declaration of competing interest

The authors declare that they have no known competing financial interests or personal relationships that could have appeared to influence the work reported in this paper.

Acknowledgments

The work of Pedro Trindade was supported by the PhD Grant 2020.04749.BD from the Fundação para a Ciência e a Tecnologia (FCT), Portugal. This work was supported by the FCT, Portugal through ISR under FCT [UIDB/50009/2020] and through the FCT, Portugal projects DECENTER [LISBOA-01-0145-FEDER-029605] and CAPTURE [PTDC/EEI-AUT/1732/2020], funded by the Lisboa 2020, Portugal and PIDDAC programs, Portugal.

Appendix A. Results used to prove Proposition 1

Lemma 5 (*Veerman & Lyons, 2020*). *Let* $\mathbf{L}$ *be the Laplacian of a strongly connected digraph. Then, for any non-negative diagonal matrix* $\mathbf{D}$ *such that* $\mathbf{D} \neq \mathbf{0}$*, all eigenvalues of* $\mathbf{L} + \mathbf{D}$ *have positive real part.*

Lemma 6 (*Veerman & Lyons, 2020*). *Any generalized Laplacian* $\boldsymbol{\mathcal{L}}$ *can be made lower block triangular by a relabeling of the vertices, where each diagonal block is the generalized Laplacian of a strongly connected digraph.*

Lemma 7. *If all eigenvalues of a generalized Laplacian* $\boldsymbol{\mathcal{L}}$ *have positive real part, then so do the eigenvalues of* $\boldsymbol{\mathcal{L}} + \mathbf{D}$*, where* $\mathbf{D}$ *is a non negative diagonal matrix.*

Proof. It follows from Lemma 6 that $\boldsymbol{\mathcal{L}}$ can be made lower block triangular, where each diagonal block $\boldsymbol{\mathcal{L}}_k$ is the generalized Laplacian of a strongly connected digraph. Note that all eigenvalues of the blocks $\boldsymbol{\mathcal{L}}_k$ have positive real part and that $\boldsymbol{\mathcal{L}}_k$ can be split as $\boldsymbol{\mathcal{L}}_k = \mathbf{L}_k + \mathbf{S}_k$, where $\mathbf{L}_k$ is the Laplacian of a strongly connected digraph and $\mathbf{S}_k$ is a non-negative diagonal matrix. It follows from Lemma 5 that $\mathbf{S}_k \neq \mathbf{0}$ and that all eigenvalues of $\boldsymbol{\mathcal{L}}_k + \mathbf{D}_k = \mathbf{L}_k + (\mathbf{S}_k + \mathbf{D}_k)$ have positive real part, and therefore all eigenvalues of $\boldsymbol{\mathcal{L}} + \mathbf{D}$ have positive real part. □

Appendix B. Proof of Proposition 1

Remark 5. The intuition for Proposition 1 comes from the interpretation of self-loops given in Section 5.1.2. For formation control, vehicles only need to have information of their state with respect to their neighbors. However, to stabilize their positions in space, absolute state information is needed. In Section 5.1.2, self-loops are used to express the knowledge a vehicle has about its absolute state. The intuition for this result is that absolute state information must flow to all vehicles in the network in order for them to achieve their desired positions. In graph theory terminology, that can be stated as follows: for any vertex j in a graph $\mathcal{G} = (\mathcal{V}, \mathcal{A})$, there must be a vertex i with a self-loop that has a directed path to j.

Taking into account the considerations of Remark 5, consider the digraph $\mathcal{G} = (\mathcal{V}, \mathcal{A})$ which is referred in the statement of Proposition 1 and let $\mathcal{V}_D \subseteq \mathcal{V}$ be the set of vertices that have a directed path to all others (which is non-empty since, by hypothesis, $\mathcal{G}$ has a spanning tree). Clearly, when a vertex $i \in \mathcal{V}_D$ has a self-loop, absolute information can flow to all vertices in the graph. An important question to raise is whether the information can reach all vertices when no vertex $i \in \mathcal{V}_D$ has a self-loop. To answer it, note that when there is a vertex $j \in \mathcal{V}_D$ and an arc $i \to j$, then it must be $i \in \mathcal{V}_D$. This means that if $i \notin \mathcal{V}_D$ and $j \in \mathcal{V}_D$ there can be no arc $i \to j$. In other words, if only vertices $i \notin \mathcal{V}_D$ have self-loops, information cannot reach the vertices $j \in \mathcal{V}_D$, meaning that there must be a vertex $i \in \mathcal{V}_D$ with a self-loop (which is in line with Proposition 1). This distinction between vertices with and without a directed path to all others motivates a partition of the matrices associated with the digraph $\mathcal{G}$, that is used to prove Proposition 1.

Proof. Consider a labeling of the vertices of $\mathcal{G}$ such that $\mathcal{V}_D = \{1, \ldots, |\mathcal{V}_D|\}$, where $|\mathcal{V}_D|$ is the number of elements in $\mathcal{V}_D$. Then, the Laplacian and the matrix of self-loop weights of $\mathcal{G}$ can be written as

$$\mathbf{L} = \begin{bmatrix} \mathbf{L}_D & \mathbf{0} \\ \mathbf{M} & \boldsymbol{\mathcal{L}}_{\bar{D}} \end{bmatrix}, \quad \text{and} \quad \mathbf{S} = \begin{bmatrix} \mathbf{S}_D & \mathbf{0} \\ \mathbf{0} & \mathbf{S}_{\bar{D}} \end{bmatrix}$$

respectively, where $\mathbf{L}_D$ is a Laplacian matrix (the rows of $\mathbf{L}$ sum to zero, therefore, so do the rows of $\mathbf{L}_D$), $\boldsymbol{\mathcal{L}}_{\bar{D}}$ is a generalized Laplacian, and $\mathbf{S}_D$ and $\mathbf{S}_{\bar{D}}$ are non-negative diagonal matrices that correspond to a splitting of $\mathbf{S}$ with dimensions that are compatible with $\mathbf{L}_D$ and $\boldsymbol{\mathcal{L}}_{\bar{D}}$.

Concretely, $\mathbf{L}_D$ is the Laplacian of a digraph $\mathcal{G}_D = (\mathcal{V}_D, \mathcal{A}_D)$, where $\mathcal{A}_D \subseteq \mathcal{A}$ contains only the arcs $i \to j \in \mathcal{A}$ such that $i, j \in \mathcal{V}_D$. Note that $\mathcal{G}_D$ is strongly connected. The block of zeros in $\mathbf{L}$ is a consequence of the fact that if $i \notin \mathcal{V}_D$ and $j \in \mathcal{V}_D$ there can be no arc $i \to j$.

Since $\mathcal{G}$ and $\mathcal{G}_D$ have a spanning tree, it follows from Lemma 1 that $\mathbf{L}$ and $\mathbf{L}_D$ have exactly one null eigenvalue and all other eigenvalues have positive real part. Recall that the eigenvalues of a block triangular matrix are the union of the eigenvalues of its diagonal blocks, to conclude that all the eigenvalues of $\boldsymbol{\mathcal{L}}_{\bar{D}}$ have positive real part.

To prove necessity, consider that no vertex $i \in \mathcal{V}_D$ has a self-loop, meaning that $\mathbf{S}_D = \mathbf{0}$. It is straightforward to conclude that $\boldsymbol{\mathcal{L}} = \mathbf{L} + \mathbf{S}$ still has a null eigenvalue associated to $\mathbf{L}_D$. Therefore, to remove the null eigenvalue from $\mathbf{L}_D$, there must be a vertex $i \in \mathcal{V}_D$ with a self-loop. Sufficiency follows from Lemma 5, since $\mathbf{L}_D$ is the Laplacian of a strongly connected digraph, and if there is a vertex $i \in \mathcal{V}_D$ with a self-loop, $\mathbf{S}_D \neq \mathbf{0}$, meaning that all eigenvalues of $\mathbf{L}_D + \mathbf{S}_D$ have positive real part. It follows from Lemma 7 that all the eigenvalues of $\boldsymbol{\mathcal{L}}_{\bar{D}} + \mathbf{S}_{\bar{D}}$ also have positive real part, and the result follows. □

Appendix C. Proof of Lemma 4

Proof. Let $\sigma := \mathrm{Re}(\eta) > 0$ and $\omega := \mathrm{Im}(\eta)$. From Lemma 3, it follows that the third degree polynomial $p_3(\lambda)$ has all its roots in the open left half-plane if and only if

$$\begin{cases} \sigma\gamma > 0 \\ \sigma^3\gamma^2 - \zeta\sigma^2\gamma + \sigma\omega^2\gamma^2 - \omega^2 > 0 \\ \zeta\left(a\zeta^2 + b\zeta + c\right) > 0 \end{cases}, \tag{C.1}$$

with $c = \left(\sigma^5 + 2\sigma^3\omega^2 + \sigma\omega^4\right)\gamma^2 - \left(\sigma^2\omega^2 + \omega^4\right)$, $a = \sigma^3$, and $b = -2\gamma\left(\sigma^4 + \sigma^2\omega^2\right)$. These conditions, however, are complex and not intuitive. In order to simplify them, some polynomial analysis can be performed. Firstly, and noting that $\sigma > 0$, the first condition becomes $\gamma > 0$. Also, in the second condition, ζ only appears in one of the terms, and thus it can be isolated, rendering the condition $\zeta < r(\gamma)$, with

$$r(\gamma) := \frac{\sigma^3\gamma^2 + \sigma\omega^2\gamma^2 - \omega^2}{\sigma^2\gamma} = \frac{\sigma^2 + \omega^2}{\sigma}\gamma - \frac{\omega^2}{\sigma^2}\frac{1}{\gamma}.$$

As for the last condition, let $p(\zeta) := a\zeta^2 + b\zeta + c$. It is straightforward to conclude that $a > 0$. Note that the roots of polynomial $p(\zeta)$ are given by

$$\zeta_{\pm}(\gamma) = \frac{\sigma^2 + \omega^2}{\sigma}\gamma \pm \frac{\sqrt{\omega^2\sigma_i^3(\sigma^2 + \omega^2)}}{\sigma^3}.$$

It can be concluded from the above expressions that the roots of $p(\zeta)$ are real. Furthermore, it is possible to conclude that $\zeta_+(\gamma) > 0$. Moreover, the sign of $\zeta_-(\gamma)$ will depend on the value of γ. The remainder of the proof is achieved by a series of contradictions.

Based on intuition, it is to expect that the condition $\zeta > 0$ must be met. Assume now that $\zeta < 0$. In order to meet the condition $\zeta\, p(\zeta) > 0$ for $\zeta < 0$, then the polynomial $p(\zeta)$ must also be negative. Since $a > 0$, then $p(\zeta)$ is negative between its roots. This means that the conditions $\zeta > \zeta_-(\gamma)$ and $\zeta < \zeta_+(\gamma)$ must be met. Since $\zeta < 0$ and $\zeta_+(\gamma) > 0$, it is clear that the condition $\zeta < \zeta_+(\gamma)$ is met. In order to be possible to have $\zeta > \zeta_-(\gamma)$, then $\zeta_-(\gamma)$ has to be negative, meaning that $\gamma < \gamma^0$, with

$$\gamma^0 := \frac{\sqrt{\omega^2\sigma^3(\sigma^2 + \omega^2)}}{\sigma^2\left(\sigma^2 + \omega^2\right)}.$$

Furthermore, to meet $\zeta < r(\gamma)$ and $\zeta > \zeta_-(\gamma)$, then $r(\gamma)$ must be bigger than $\zeta_-(\gamma)$. Hence,

$$r(\gamma) - \zeta_-(\gamma) = \frac{\sqrt{\omega^2\sigma^3(\sigma^2 + \omega^2)}}{\sigma^3} - \frac{\omega^2}{\sigma^2}\frac{1}{\gamma}, \tag{C.2}$$

must be bigger than zero. However, considering that $\gamma < \gamma^0$, the following conclusion can be drawn about (C.2)

$$r(\gamma) - \zeta_-(\gamma) < \frac{\sqrt{\omega^2\sigma^3(\sigma^2 + \omega^2)}}{\sigma^3} - \frac{\omega^2}{\sigma^2}\frac{1}{\gamma^0} = 0.$$

Thus, it is concluded that $\zeta < 0$ is not a solution to the set of conditions previously described.

Considering now that $\zeta > 0$, in order to verify the condition $\zeta\, p(\zeta) > 0$, the polynomial $p(\zeta)$ must be also be positive. Since $a > 0$, it is known that this happens outside the roots of $p(\zeta)$, which means that $\zeta < \zeta_-(\gamma)$ or $\zeta > \zeta_+(\gamma)$. However, the possibility of $\zeta > \zeta_+(\gamma)$ is quickly discarded since it is straightforward to conclude that $\zeta_+(\gamma) > r(\gamma)$, meaning that the condition $\zeta > \zeta_+(\gamma)$ is not compatible with condition $\zeta < r(\gamma)$. Hence, the solution that remains is to have $\zeta < \zeta_-(\gamma)$. Note that ζ is positive. Thus, in order for this condition to be possible, $\zeta_-(\gamma)$ must be positive. It is now possible to conclude that in order to have $\zeta_-(\gamma) > 0$, then $\gamma > \gamma^0$. Note that this is more conservative than having $\gamma > 0$ because $\gamma^0 \geq 0$, hence the condition $\gamma > 0$ can be dropped.

It is now left to verify which of the conditions, $\zeta < \zeta_-(\gamma)$ or $\zeta < r(\gamma)$, is the most conservative. Considering that it must be $\gamma > \gamma_0$, it follows that

$$r(\gamma) - \zeta_-(\gamma) > \frac{\sqrt{\omega^2\sigma^3(\sigma^2 + \omega^2)}}{\sigma^3} - \frac{\omega^2}{\sigma^2}\frac{1}{\gamma^0} = 0. \tag{C.3}$$

Therefore, $r(\gamma) > \zeta_-(\gamma)$, hence concluding that the condition $\zeta < \zeta_-(\gamma)$ is the most conservative. Finally, considering $\omega_n = |\eta| = \sqrt{\sigma^2 + \omega^2}$ and $\xi = \frac{\sigma}{\omega_n}$, it follows that

$$\begin{cases} \gamma > \gamma^0 = \sqrt{\frac{1-\xi^2}{\xi\omega_n}} \\ 0 < \zeta < \zeta_-(\gamma) = \left[\frac{\omega_n}{\xi}\left(\gamma - \sqrt{\frac{1-\xi^2}{\xi\omega_n}}\right)\right] \end{cases},$$

hence concluding the proof. □

References

Ahn, H. S. (2020). *Studies in systems, decision and control: vol. 205, Formation control: Approaches for distributed agents* (1st ed.). Springer, http://dx.doi.org/10.1007/978-3-030-15187-4.

Cao, Y., & Sun, Y. (2014). Necessary and sufficient conditions for consensus of third-order multi-agent systems. In *Proceedings of the 14th international conference on control, automation and systems* (pp. 895–900). http://dx.doi.org/10.1109/ICCAS.2014.6987911.

Falanga, D., Kim, S., & Scaramuzza, D. (2019). How fast is too fast? The role of perception latency in high-speed sense and avoid. *IEEE Robotics and Automation Letters*, *4*(2), 1884–1891. http://dx.doi.org/10.1109/LRA.2019.2898117.

Fax, J. A., & Murray, R. M. (2004). Information flow and cooperative control of vehicle formations. *IEEE Transactions on Automatic Control*, *49*(9), 1465–1476. http://dx.doi.org/10.1109/TAC.2004.834433.

Frank, E. (1946). On the zeros of polynomials with complex coefficients. *Bulletin of the American Mathematical Society*, *52*(2), 144–157. http://dx.doi.org/10.1090/S0002-9904-1946-08526-2.

Han, L., Dong, X., Li, Q., & Ren, Z. (2017). Formation tracking control for time-delayed multi-agent systems with second-order dynamics. *Chinese Journal of Aeronautics*, *30*(1), 348–357. http://dx.doi.org/10.1016/j.cja.2016.10.019.

Huang, C., Zhai, G., & Xu, G. (2018). Necessary and sufficient conditions for consensus in third order multi-agent systems. *IEEE/CAA Journal of Automatica Sinica*, *5*(6), 1044–1053. http://dx.doi.org/10.1109/JAS.2018.7511222.

Krick, L., Broucke, M., & Francis, B. (2008). Stabilization of infinitesimally rigid formations of multi-robot networks. In *47th IEEE conference on decision and control, vol. 82* (pp. 477–482). http://dx.doi.org/10.1109/CDC.2008.4738760.

Mukherjee, D., & Zelazo, D. (2019). Consensus of higher order agents: Robustness and heterogeneity. *IEEE Transactions on Control of Network Systems*, *6*(4), 1323–1333. http://dx.doi.org/10.1109/TCNS.2018.2889003.

Oh, K. K., & Ahn, H. S. (2014). Distance-based undirected formations of single-integrator and double-integrator modeled agents in n-dimensional space. *International Journal of Robust and Nonlinear Control*, *24*(12), 1809–1820. http://dx.doi.org/10.1002/rnc.2967.

Oh, K. K., Park, M. C., & Ahn, H. S. (2015). A survey of multi-agent formation control. *Automatica*, *53*, 424–440. http://dx.doi.org/10.1016/j.automatica.2014.10.022.

Olfati-Saber, R., & Murray, R. M. (2004). Consensus problems in networks of agents with switching topology and time-delays. *IEEE Transactions on Automatic Control*, *49*(9), 1520–1533. http://dx.doi.org/10.1109/TAC.2004.834113.

Ren, W., & Atkins, E. (2007). Distributed multi-vehicle coordinated control via local information exchange. *International Journal of Robust and Nonlinear Control*, *17*(10–11), 1002–1033. http://dx.doi.org/10.1002/rnc.1147.

Ren, W., Beard, R., & McLain, T. (2004). Coordination variables and consensus building in multiple vehicle systems. In *Proceedings of the block island workshop on cooperative control, vol. 309* (pp. 439–442). http://dx.doi.org/10.1007/978-3-540-31595-7_10.

Ren, W., Moore, K., & Chen, Y. (2006). High-order consensus algorithms in cooperative vehicle systems. In *Proceedings of the IEEE international conference on networking, sensing and control* (pp. 457–462). http://dx.doi.org/10.1109/ICNSC.2006.1673189.

Ren, W., Moore, K., & Chen, Y. (2007). High-order and model reference consensus algorithms in cooperative control of MultiVehicle systems. *Journal of Dynamic Systems, Measurement, and Control*, *129*(5), 678–688. http://dx.doi.org/10.1115/1.2764508.

Tang, Z., Cunha, R., Hamel, T., & Silvestre, C. (2021). Formation control of a leader–follower structure in three dimensional space using bearing measurements. *Automatica*, *128*, http://dx.doi.org/10.1016/j.automatica.2021.109567.

Tegling, E., Bamieh, B., & Sandberg, H. (2019). Localized high-order consensus destabilizes large-scale networks. In *Proceedings of the 2019 American control conference* (pp. 760–765). http://dx.doi.org/10.23919/ACC.2019.8815369.

Trindade, P., Cunha, R., & Batista, P. (2020). Distributed formation control of double-integrator vehicles with disturbance rejection. *IFAC-PapersOnLine*, *53*(2), 3118–3123. http://dx.doi.org/10.1016/j.ifacol.2020.12.1045, 21th IFAC World Congress.

V. Dimarogonas, D., & Johansson, K. (2008). On the stability of distance-based formation control. In *Proceedings of the IEEE conference on decision and control* (pp. 1200–1205). http://dx.doi.org/10.1109/CDC.2008.4739215.

Veerman, J. J. P., & Lyons, R. (2020). A primer on Laplacian dynamics in directed graphs. *Nonlinear Phenomena in Complex Systems*, *23*(2), 196–206. http://dx.doi.org/10.33581/1561-4085-2020-23-2-196-206.

Yu, W., Chen, G., & Cao, M. (2010). Some necessary and sufficient conditions for second-order consensus in multi-agent dynamical systems. *Automatica*, *46*(6), 1089–1095. http://dx.doi.org/10.1016/j.automatica.2010.03.006.

Zhao, S., & Zelazo, D. (2017). Translational and scaling formation maneuver control via a bearing-based approach. *IEEE Transactions on Control of Network Systems*, *4*(3), 429–438. http://dx.doi.org/10.1109/TCNS.2015.2507547.

Zhu, J., Tian, Y.-P., & Kuang, J. (2009). On the general consensus protocol of multi-agent systems with double-integrator dynamics. *Linear Algebra and its Applications*, *431*(5), 701–715. http://dx.doi.org/10.1016/j.laa.2009.03.019.